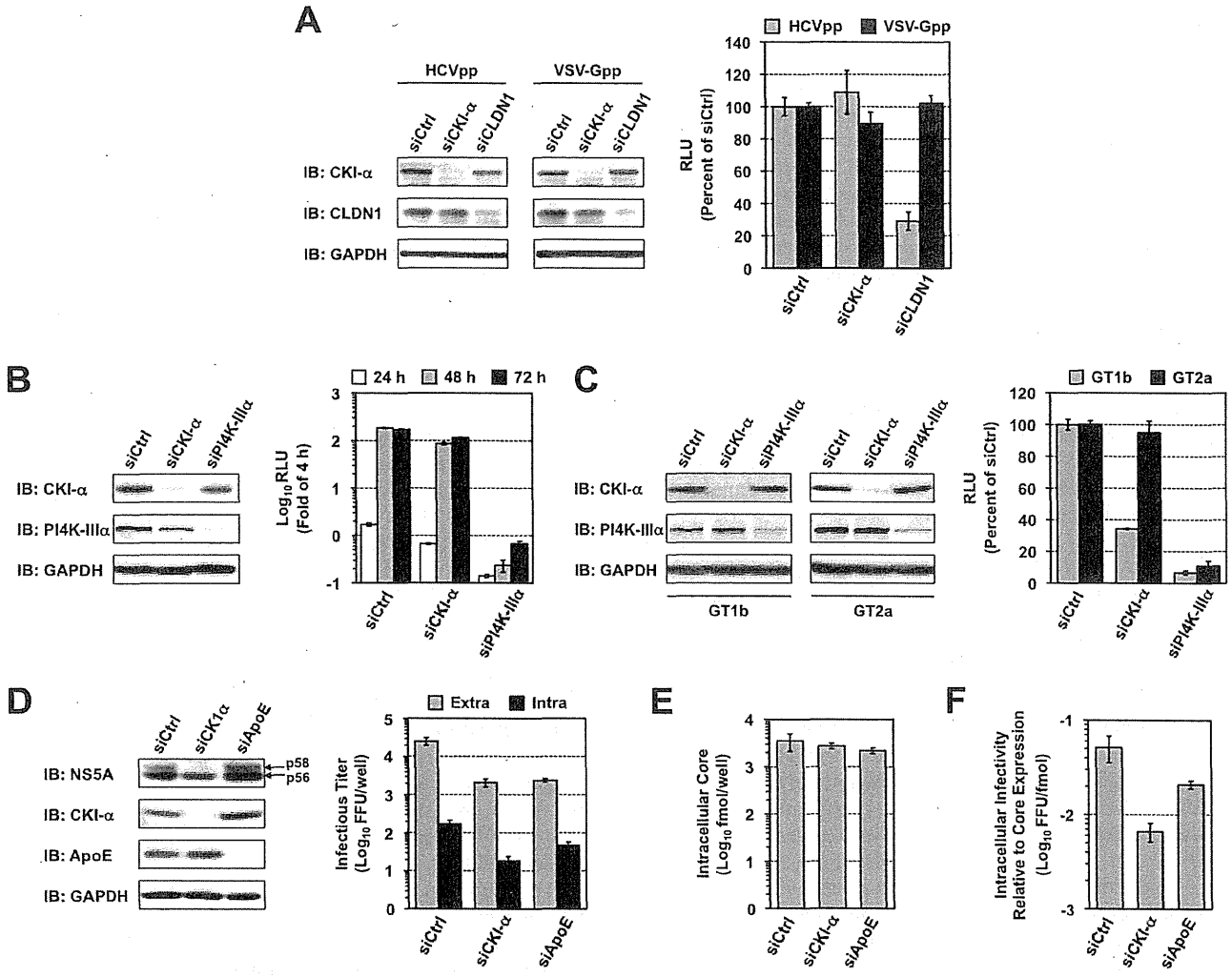

FIG 4 Virion assembly is a primary target of CKI-α. (A) Effect of CKI-α knockdown on viral entry. Huh7.5.1 cells were transfected with the indicated siRNAs. Two days later, cells were infected with HCVpp (gray bars) or VSV-Gpp (black bars) and harvested an additional 3 days later for immunoblotting (IB) and luciferase assays. Values were normalized to the value for transfection with control siRNAs (siCtrl), set at 100%. Values shown represent the means ± standard deviations from three independent transfections of siRNA. (B) Transient replication assay for the JFH-1 subgenomic replicon following CKI-α knockdown. Huh-7 cells transfected with the indicated siRNAs were coelectroporated with the identical siRNAs, and JFH-1 subgenomic luciferase reporter replicon RNA, and harvested at the indicated time points for immunoblotting (IB) and luciferase assays. The luciferase activity at each time point was corrected by the luciferase value at 4 h posttransfection to normalize transfection efficiencies. Values shown represent the means ± standard deviations from three replicate experiments. (C) Effects of CKI-α knockdown on replication in replicon cell lines derived from genotypes 1b and 2a. Two cell lines harboring an HCV subgenomic luciferase reporter replicon, LucNeo#2 (genotype 1b, GT1b) and SGR-JFH1/LucNeo (genotype 2a, GT2a), were transfected with the indicated siRNAs and harvested 3 days later for immunoblotting (IB) and luciferase assays. Luciferase activities were normalized to the luciferase values for transfection with control siRNA (siCtrl), set at 100%. Values shown represent the means ± standard deviations from three independent transfections of siRNA. (D) Effects of CKI-α knockdown on viral assembly and release. Huh7-25 cells transfected with the indicated siRNAs were coelectroporated with the identical siRNAs and JFH-1 RNA. Cells and supernatants were harvested 3 days later for immunoblotting (IB) and titrations of extracellular and intracellular infectious virus by focus-forming unit (FFU) assays. Values represent the means ± standard deviations from three replicate experiments. (E) Effect of CKI-α knockdown on the abundance of intracellular core protein. Amounts of core in cells for which results are shown in panel D were measured. Results represent the means ± standard deviations from three replicate experiments. (F) Effect of CKI-α knockdown on intracellular infectivity relative to core protein expression. Intracellular infectivity relative to core expression was determined by normalizing the yield of intracellular infectious virus (shown in panel D) with the amount of intracellular core protein shown in panel E. Results represent the means ± standard deviations from three replicate experiments.

followed by harvesting at different time points (Fig. 4B). The reporter luciferase activity at each time point was corrected with the luciferase value at 4 h posttransfection to normalize transfection efficiencies. Although efficient knockdown was achieved with siRNAs (Fig. 4B, left panel), CKI-α knockdown led to a marginal but nonnegligible decrease in the luciferase activity over the indicated time period. In contrast, PI4K-IIIα knockdown, as a positive control, resulted in a marked decrease (>200-fold) in activity (Fig. 4B, right panel). The effect of CKI-α silencing on the replication of the subgenomic replicon was further analyzed by using two cell lines derived from genotype 1b (LucNeo#2) (38, 39) and genotype 2a (SGR-JFH1/LucNeo) (Fig. 4C). Both Huh-7-based

subgenomic replicon cell lines carry a firefly luciferase reporter gene fused to the neomycin phosphotransferase gene. As shown in the right panel of Fig. 4C, knockdown of CKI-α resulted in a marked (~65%) decrease in replication of the genotype 1b replicon but only a slight (~10%) decrease in the genotype 2a replication, although knockdown efficiencies of CKI-α were sufficient and comparable in both cell lines (Fig. 4C, left panels). Our result with the genotype 1b replicon was consistent with a previous report (27). In contrast, the limited impact of CKI-α silencing on the replication of the JFH-1 subgenomic replicon suggests that the RNA replication step may not be a key role for CKI-α in the regulation of HCV JFH-1 production.

Finally, we focused on the late stages of the HCV life cycle and analyzed the involvement of CKI-α in virion assembly and release via a single-cycle virus production assay (55), in which Huh7–25 cells lacking CD81 expression were used. Three days posttransfection with siRNAs, the cells were cotransfected with the identical siRNAs and JFH-1 RNA by electroporation. The cells and culture supernatants were harvested after a further 3 days, and titrations of intra- and extracellular infectious virus were assessed (Fig. 4D to F). Reduced NS5A hyperphosphorylation was observed following CKI-α knockdown, but not following ApoE knockdown or transfection with irrelevant siRNA (Fig. 4D, left panel). Both CKI-α and ApoE knockdown led to an ~10-fold reduction in the yield of extracellular infectious virus compared to the negative control. Approximately a 9-fold reduction was found in the yield of intracellular infectious virus following CKI-α knockdown (Fig. 4D, right panel), indicating that CKI-α is not required for virus release from cells. Despite the marked decrease in intracellular virion yield, CKI-α knockdown resulted in only a 1.3-fold reduction in the abundance of intracellular core protein (Fig. 4E), supporting a limited impact for CKI-α knockdown on viral replication (Fig. 4B). Furthermore, CKI-α silencing led to approximately an 8-fold reduction in the intracellular infectivity relative to core protein expression, which represents the efficiency of viral assembly expressed as the yield of intracellular infectious virus normalized to the amount of intracellular core protein (Fig. 4F). Collectively, these observations suggest that in the HCV life cycle, CKI-α plays a key role most likely in the assembly of infectious viral particles.

NS5A hyperphosphorylation mediated by CKI-α possibly contributes to recruitment of NS5A to low-density membrane structures around LDs in infected cells. It has been demonstrated that recruitment of NS5A to cytoplasmic low-density membrane structures surrounding LDs, and the interaction of NS5A with the core protein at the site, are essential to HCV assembly (7, 8, 56). To gain mechanistic insight into the function of CKI-α in virion assembly, we performed a subcellular fractionation assay and examined whether NS5A phosphorylation by CKI-α contributed to the subcellular localization of NS5A. Lysates of cells transfected with JFH-1 RNA in the presence or absence of CKI-α silencing (Fig. 5A, left panel) were fractionated with 2.5 to 30% iodixanol gradients followed by immunoblotting of the fractions (Fig. 5A, right panels). In control cells (siCtrl), hyperphosphorylated p58 NS5A predominantly resided in low-density fractions, such as fractions 1 to 3, while hypophosphorylated p56 NS5A localized not only in the low-density fractions but also in high-density fractions, such as fractions 11 and 12. In contrast, knockdown of CKI-α (siCKI-α) decreased the abundance of hyperphosphorylated NS5A and NS5A in the low-density fractions. NS5A levels in the high-density fractions were not reduced by CKI-α knockdown. These results indicate that CKI-α is involved in the distribution of NS5A in cells as well as in its hyperphosphorylation.

We next assessed whether the intracellular localization of NS5A and its interaction with LDs or the core protein are affected by CKI-α knockdown by using laser-scanning confocal immunofluorescence microscopy. Cells were transfected either with CKI-α siRNA (siCKI-α) or with an irrelevant control siRNA (siCtrl), followed by infection with HCVcc. Efficient knockdown of CKI-α was confirmed by immunoblotting and was associated with decreased p58 expression (Fig. 5B). The delivery of siRNA into nearly 100% of the cells was observed with Cy3-labeled siRNA (Silencer Cy3-labeled GAPDH siRNA) (Fig. 5C). In siCtrl-transfected cells, NS5A was colocalized or closely associated with LDs. In contrast, its association with LDs was decreased following CKI-α depletion (Fig. 5D) ($P < 0.0001$ by two-sided Mann-Whitney test). Similarly, NS5A and the core protein were clearly colocalized in control cells, while their colocalization was reduced in CKI-α knockdown cells (Fig. 5E) ($P = 0.0110$ by two-sided Mann-Whitney test). These microscopy findings suggest that CKI-α and/or CKI-α-mediated hyperphosphorylation of NS5A is involved in the NS5A-core colocalization at or around LDs in HCV-infected cells. Taken together with the results of our subcellular fractionation assay (Fig. 5A), it is likely that CKI-α plays a role in recruiting NS5A to low-density membrane structures around LDs through hyperphosphorylation of NS5A, and it may facilitate the NS5A-core interaction at these sites.

Identification of potential phospho-acceptor regions for CKI-α. The above results prompted us to identify the phospho-acceptor sites for CKI-α by using a proteomics approach. Lysates of cells expressing the HCV JFH-1 genome, transfected with either CKI-α siRNA or an irrelevant control siRNA, were immunoprecipitated with an anti-NS5A antibody followed by SDS-PAGE (Fig. 6A). Immunoblotting showed a marked reduction of NS5A p58 following CKI-α knockdown (Fig. 6A, right panel). Silver-stained gel bands of p58 and p56 (Fig. 6A, left panel) were excised and subjected to in-gel digestion, followed by mass spectrometry analysis (Fig. 6B). A total of 629 peptides were identified from both control NS5A (siCtrl) and NS5A with CKI-α knockdown (siCKI-α) after peptide selection with a Mascot peptide score of ≥25 (see Table S3 in the supplemental material) and yielded 53% proteome coverage in total (49.4% for control NS5A and 41.8% for NS5A with CKI-α knockdown), as indicated in the upper panel of Fig. 6B (red letters). Peptides corresponding to domain III in NS5A were not obtained in this analysis. We identified three kinds of phosphopeptides (1, GSPPSEASSSVSQLSAPSLR; 2, APTPPPR; 3, TVGLSESTISEALQQLAIK [Fig. 6B, upper panel, highlighted in green, blue, and yellow, respectively]) (see also Table S3). However, fine mapping of phosphorylation sites was not completely successful in this assay, probably due to the low abundance of immunoprecipitated NS5A. We next assessed which peptide contained the potential phospho-acceptor sites for CKI-α by comparing the frequencies of phosphopeptides identified with and without CKI-α knockdown. As shown in the lower panel of Fig. 6B, the frequency of phosphopeptide 1 relative to the total number of peptide 1 identified was decreased after CKI-α knockdown (from 26.2% to 19.8%). In contrast, the relative frequencies of phosphopeptides 2 and 3 were unaffected or increased by CKI-α knockdown. We noted that the threonine residue in peptide 2 is unlikely to be a consensus phosphorylation site of CKI

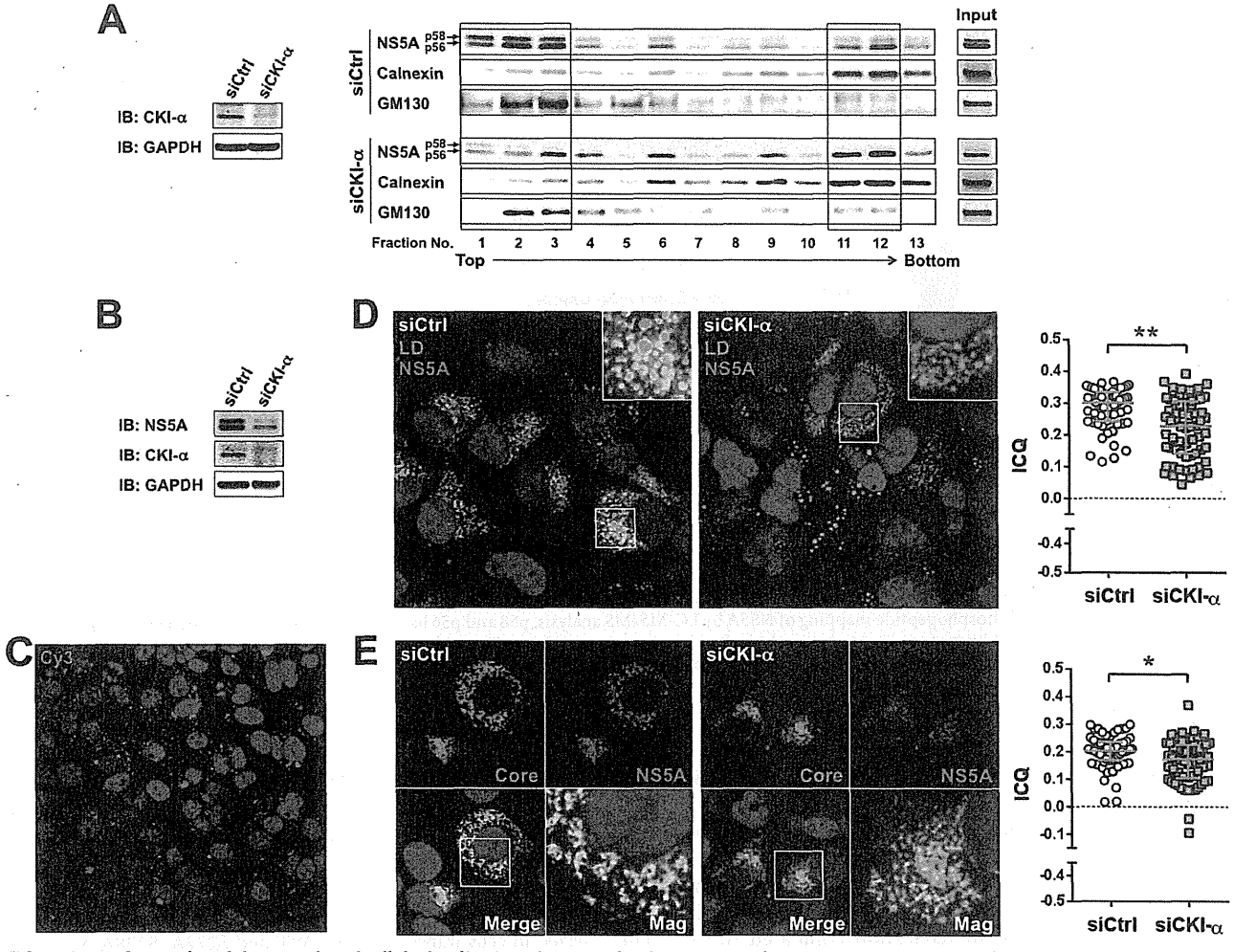

FIG 5 Effects of CKI-α knockdown on the subcellular localization of NS5A and its interaction with LDs or core protein. (A) Iodixanol density gradient analysis (right). Huh7-25 cells transfected with the indicated siRNAs were coelectroporated with the identical siRNAs and JFH-1 RNA. Cell lysates were prepared 3 days after electroporation and fractionated by iodixanol gradients of 2.5% to 30%. The gradient was collected in 0.8-ml fractions for immunoblotting. Total cell lysates before fractionation were loaded as input controls. Detected bands in fractions 1 to 3 and in fractions 11 and 12 are enclosed by squares. (Left) Immunoblotting (IB) results for CKI-α 3 days after electroporation. GAPDH was included as a loading control. (B) Immunoblot (IB) of NS5A and CKI-α 3 days after HCVcc infection. GAPDH was included as a loading control. (C) siRNA delivery efficiency. Cy3 fluorescence (red) was observed 3 days after transfection of Silencer Cy3-labeled GAPDH siRNA. Nuclei were counterstained with Hoechst 33342 (blue). (D) Colocalization of NS5A and LDs. Confocal microscopy images show cells transfected with either CKI-α siRNA (siCKI-α) or an irrelevant control siRNA (siCtrl), followed by infection with JFH-1 virus (left). Cells were fixed with paraformaldehyde 3 days after infection and labeled with an antibody specific for NS5A (red). Cells were counterstained with BODIPY 493/503 (green) to label lipid droplets and with Hoechst 33342 (blue) to label nuclei. Insets represent enlarged views of portions surrounded by squares. Colocalization of NS5A and LDs pixels were assessed quantitatively by intensity correlation analysis using ImageJ software (right). Plots shown represent the ICQ obtained from each of >60 NS5A/LD double-positive cells. Bars indicate the median ± interquartile range of the plots. **, $P < 0.01$ by two-sided Mann-Whitney test. (E) Colocalization of NS5A and core protein. Confocal microscopy images show cells transfected either with CKI-α siRNA (siCKI-α) or with a control siRNA (siCtrl), followed by infection with JFH-1 virus (left). Fixed cells were labeled with antibodies specific for NS5A (red) and core (green). Nuclei were counterstained with Hoechst 33342 (blue) in the merged images. Mag images represent enlarged views of portions surrounded by squares in the merged images. Colocalization of NS5A and core pixels was assessed quantitatively by intensity correlation analysis using ImageJ software (right). Plots shown represent ICQs obtained from each of >60 NS5A/core double-positive cells. Bars indicate the median ± interquartile range. *, $P < 0.05$ by two-sided Mann-Whitney test.

(57). Thus, the results suggest that peptide 1 (GSPPSEASSSVSQL SAPSLR) is the peptide most likely to contain the amino acids phosphorylated by CKI-α.

S225 and S232 are key residues involved in NS5A hyperphosphorylation and hyperphosphorylation-dependent regulation of infectious virus production. Peptide 1 identified above contains eight serine residues that are highly conserved among HCV isolates and are clustered within LCS I (Fig. 7A). To identify amino acids responsible for CKI-α-mediated hyperphosphorylation, we assessed the impacts of alanine or aspartic acid substitutions for these 8 serine residues on NS5A hyperphosphorylation and virus production. An HCV JFH-1 genome with the reporter luciferase, which enabled us to evaluate viral replication by measuring GLuc activity, and a series of its NS5A mutated constructs (Fig. 7A) were generated. Supernatants of cell cultures transfected with the RNA transcripts were harvested at 4, 24, 48, and 72 h posttransfection

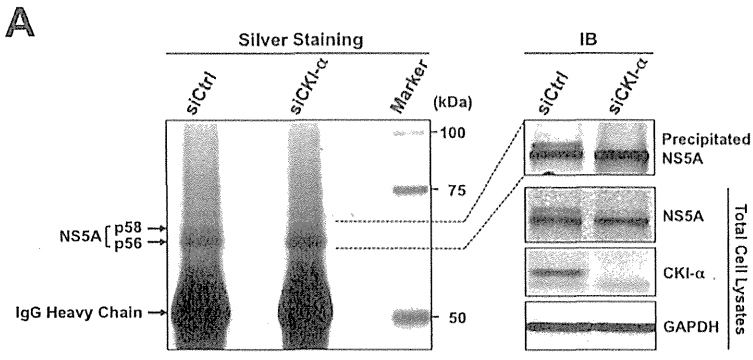

B

```
  1 SGSWLRDVWDWVCTILTDFKNWLTSKLFPKLPGLPFISCQ  40
 41 KGYKGVWAGTGIMTTRCPCGANISGNVRLGSMRITGPKTC  80
 81 MNTWQGTFPINCYTEGQCAPKPPTNYKTAIWRVAASEYAE 120
121 VTQHGSYSYVTGLTTDNLKIPCQLPSPEFFSWVDGVQIHR 160
161 FAPTPKPFFRDEVSFCVGLNSYAVGSQLPCEPEPDADVLR 200
201 SMLTDPPHITAETAARRLAR                      240
241 ATCTTHSNTYDVDMVDANLLMEGGVAQTEPESRVPVLDFL 280
281 EPMAEEESDLEPSIPSECMLPRSGFPRALPAWARPDYNPP 320
321 LVESWRRPDYQPPTVAGCALPPPKKAPTPPPRRRRTVGLS 360
361 ESTISEALQQLAIKTFGQPPSSGDAGSSTGAGAAESGGPT 400
401 SPGEPAPSETGSASSMPPLEGEPGDPDLESDQVELQPPPQ 440
441 GGGVAPGSGSGSWSTCSEEDDTTVCC               466
```

Peptides Identified		No. of Peptides Identified Phospho/Total siCtrl	siCKI-α
#1	GSPPSEASSS VSQLSAPSLR	17/65 (26.2%)	18/91 (19.8%)
#2	APTPPPR	16/28 (57.1%)	14/21 (66.7%)
#3	TVGLSESTIS EALQQLAIK	1/16 (0.1%)	1/14 (0.1%)

FIG 6 Identification of NS5A phosphopeptides by a phospho-proteome approach. (A) Silver staining and immunoblotting of immunoprecipitated NS5A. Huh-7 cells transfected with the indicated siRNAs were coelectroporated with the identical siRNAs and JFH-1 RNA. Cell lysates were prepared 3 days after electroporation and immunoprecipitated with an anti-NS5A antibody. Immunoprecipitates were subjected to SDS-PAGE, followed by silver staining and immunoblotting (IB). (B) Phosphopeptide mapping of NS5A by LC-MS/MS analysis. p58 and p56 bands of NS5A were excised from the gel and subjected to in-gel digestion, followed by mass spectrometry analysis. Red letters represent the amino acids identified. Three kinds of phosphopeptides identified are highlighted in green (phosphopeptide 1), blue (phosphopeptide 2), and yellow (phosphopeptide 3). The numbers represent amino acid positions within NS5A.

and subjected to the GLuc assay. As shown in the left panel of Fig. 7B, serine-to-alanine substitution at either aa 229 (S229A) or at aa 235 (S235A) resulted in severe reduction in the viral replication. In contrast, the replication capacities of S222A, S228A, S230A, and S238A mutant reporter viruses were comparable to that of the wild type (WT). S225A and S232A mutations led to a slight but nonnegligible reduction in replication compared to WT. The phospho-mimetic aspartic acid substitution for aa 235 (S235D) exhibited a much higher replication capacity (~100-fold) than S235A, indicating that phosphorylation of S235 is required for efficient viral replication. In contrast, the replication capacity of S229D was still more-than-10-fold lower than that of WT, suggesting that introduction of negative charge at this position is not sufficient to enhance viral replication (Fig. 7B, right panel). S225D and S232D mutations restored viral replication capacities and exhibited the same replication phenotype as WT. Interestingly, S222D and S230D resulted in a slight reduction in viral replication compared to S222A and S230A, consistent with previous reports (23, 58) (Fig. 7B, right panel).

We next evaluated the effects of the NS5A mutations on infectious virus production by titrations of infectious virus in culture supernatants of cells transfected with RNA transcripts of JFH-1 viruses at 72 h posttransfection (Fig. 7C). S225A and S232A mutations resulted in 4- and 5-fold reductions in the virus infectious titer, respectively, compared to WT, while the abilities of S225D and S232D mutants to produce infectious virus were comparable to that of WT. Little or no virus production was observed with S229A, S229D, and S235A mutations, presumably because of their strong negative impacts on viral replication. A slight reduction in virus production observed with S230D and S235D mutations was most likely due to their replication capacities. S222A, S222D, S228A, S228D, S230A, S238A, and S238D substitutions had no significant effect on virus production (>75% of the WT level).

To determine the effect of the NS5A mutations on NS5A hyperphosphorylation, cells expressing JFH-1 viruses were subjected to immunoblotting, and the p58/p56 ratio of NS5A was estimated (Fig. 7D). The hyperphosphorylated p58 band of NS5A was clearly detected in cells transfected with WT and S222A, S228A, S230A, and S238A mutants, which had mean p58/p56 ratios of 0.42, 0.38, 0.35, 0.50, and 0.60, respectively. These p58/p56 ratios were reproducible in multiple repeated experiments but much lower than the p58/p56 ratios (e.g., 0.93 in siCtrl-transfected cells) in Fig. 3A. This difference may be attributed to the difference in the way by which HCV was introduced into cells (virus infection in Fig. 3A and transfection of viral genome in Fig. 7D and F). The p58 levels were significantly reduced in cells transfected with S225A or S232A mutants, which had mean p58/p56 ratios of 0.11 and 0.15, respectively (Fig. 7D). Since the p58/p56 ratios of the S229A and S235A mutants were not determined due to low levels of NS5A expression, we reevaluated the p58/p56 ratio of each viral muatant by using a vaccinia virus-T7 polymerase-mediated protein expression system (Fig. 7E, left panel). Cells transfected with pJFH1 or a series of its NS5A mutants were infected with vaccinia virus expressing the T7 RNA polymerase and harvested for immunoblotting. Similar to the results shown in Fig. 7D, the p58/p56 ratios of S225A and S232A mutants were significantly reduced, while S229A and S235A mutations had no effects (Fig. 7E, right panel). The hyperphosphorylated band of NS5A was observed in cells transfected with the S222D, S225D, S228D, S229D, or S230D mutant in both experimental settings. Interestingly, the S232D, S235D, and S238D mutations resulted in a slight retardation of p56 mobility (Fig. 7F and G), consistent with previous reports (58, 59).

Collectively, S225 and S232 are key residues involved in

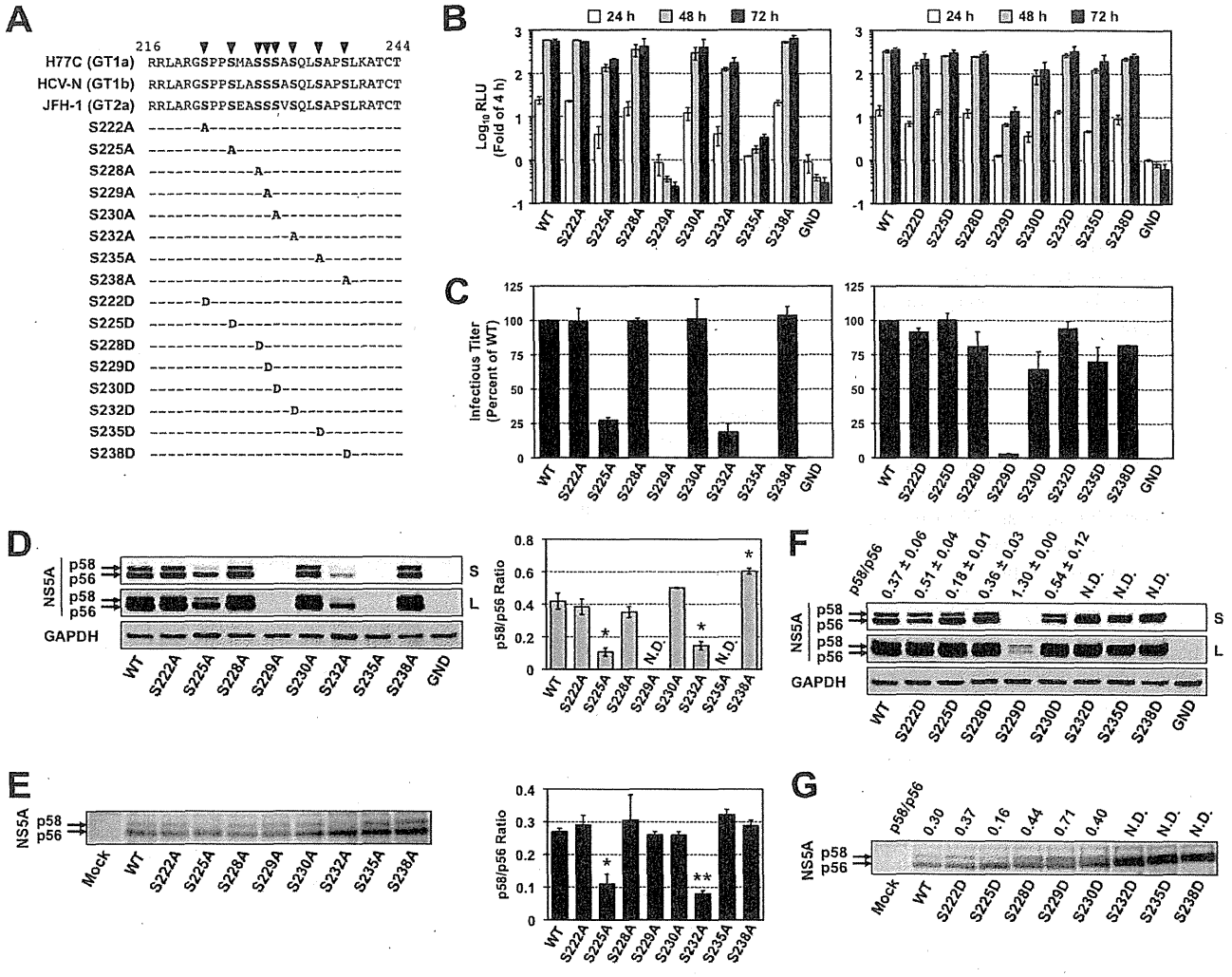

FIG 7 Effects of mutations at potential CKI-α phosphorylation sites on NS5A hyperphosphorylation, viral replication, and infectious virion production. (A) Highly conserved serine residues located within the LCS I region of NS5A and the sequences of NS5A mutants used. Arrowheads represent putative phosphorylation sites replaced with alanine or aspartic acid. The numbers represent amino acid positions within NS5A. (B) Viral replication. Huh-7 cells were transfected with the indicated JFH-1-based GLuc reporter constructs, including the WT and its replication-defective mutant (GND). Culture supernatants were harvested at the indicated time points for luciferase assays. The GLuc activity at each time point was normalized with the activity at 4 h posttransfection, and the fold chnages are shown. Results represent the means ± standard deviations from three independent experiments, each performed in triplicate. (C) Infectious virion production. Huh-7 cells were transfected with the indicated JFH-1 viral RNAs, including the WT and its replication-defective mutant (GND). Culture supernatants were harvested 3 days (72 h) later for titrations of infectious virus in a focus-forming unit (FFU) assay. The infectious virus yield of each NS5A mutant was normalized with that of JFH-1 WT, which was set at 100%. Results represent the means ± standard deviations from multiple independent experiments, each performed at least in triplicate. (D) Immunoblot of NS5A in lysates of cells transfected with JFH-1 viral RNAs carrying the indicated serine-to-alanine mutations (left). GAPDH is a loading control. The p58/p56 ratio of each virus was determined by carrying out densitometric analysis of NS5A bands (right). Results shown represent the means ± standard deviations from multiple independent experiments. *, $P < 0.05$, compared to WT. N.D., not determined, due to low levels of expression. (E) Vaccinia virus-T7 polymerase-mediated expression of NS5A in cells transfected with pJFH1 carrying the indicated serine-to-alanine mutations (left). NS5A bands were quantified by densitometric analysis, and p58/p56 ratios were calculated (right). Data shown represent the means ± standard deviations from multiple independent experiments. *, $P < 0.05$; **, $P < 0.01$ (versus WT). (F) Immunoblot of NS5A in lysates of cells transfected with JFH-1 viral RNA carrying the indicated serine-to-aspartic acid mutation. GAPDH was included as a loading control. The p58/p56 ratio of each virus was determined by carrying out densitometric analysis of NS5A bands. Results shown represent the means ± standard deviations from multiple independent experiments. N.D., not determined, due to the poor separation of p58 and p56 bands. (G) Vaccinia virus-T7 polymerase-mediated expression of NS5A in cells transfected with pJFH1 carrying the indicated serine-to-aspartic acid mutation. NS5A bands were quantified by densitometric analysis, and p58/p56 ratios were calculated. Data shown are representative of two independent experiments. N.D., not determined, due to the poor separation of p58 and p56 bands. S and L in panels D and F represent short exposure and long exposure, respectively.

NS5A hyperphosphorylation and hyperphosphorylation-dependent regulation of infectious virus production. In addition, S225A and S232A reproduced the viral phenotype following CKI-α knockdown more precisely than the other serine mutants within the peptide 1 region. It is most likely that S225 and S232 of NS5A are important for CKI-α-mediated hyperphosphorylation, which is involved in the robust production of infectious HCV.

DISCUSSION

Phosphorylation at serine and threonine residues in HCV NS5A is critical for regulation of the viral life cycle, including genome replication and infectious virus assembly (8, 9, 14, 16–18, 59–61). Several serine/threonine protein kinases have been identified as enzymes that potentially phosphorylate NS5A (9, 25, 26, 28, 50, 51). To our knowledge, however, this study is the first to identify through a kinome-wide screening protein kinases that interact with and phosphorylate NS5A. The *in vitro* AlphaScreen and phosphorylation assays, followed by RNAi screening on the HCVcc system, identified CKI-α as a major NS5A-associated kinase involved in NS5A hyperphosphorylation and the production of infectious virus.

In a previous study, CKI-α was reported to be involved in the replication of the subgenomic replicon derived from genotype 1b, with evidence that attenuation of CKI-α expression inhibited viral RNA replication up to 60% 5 days after the CKI-α knockdown (27). However, our study with the HCVcc system, as well as detailed analyses dissecting individual steps in the HCV life cycle, revealed that virion assembly is more affected by CKI-α silencing than is viral genome replication. It is highly likely that the CKI-α-mediated hyperphosphorylation of NS5A plays a role in recruiting NS5A to low-density membrane structures around LDs, leading to the acceleration of the early step(s) of virus particle formation. Mutagenesis analyses of putative CKI-α phosphorylation sites identified by a phospho-proteomic approach demonstrated that serine-to-alanine substitution at aa 225 or aa 232 in NS5A did to some extent reproduce the viral phenotype following CKI-α knockdown, indicating that S225 and S232 may be key residues for CKI-α-mediated NS5A hyperphosphorylation and regulation of virion assembly.

It is commonly held that HCV replication is regulated through the tight and delicate control of the ratio between p58 and p56 levels. Adaptive mutations or kinase inhibitors, which reduce NS5A hyperphosphorylation, enhance the HCV RNA replication of genotype 1 isolates, possibly by modulating its interaction with the host vesicle-associated membrane protein-associated protein subtype A (VAP-A), which is an essential factor for HCV replication (17–19, 24). In contrast, reduction of NS5A hyperphosphorylation by RNAi targeting protein kinases results in inhibition of the replication of genotype 1 adaptive replicons, indicating a role for p58 in efficient viral replication (25, 27). Impaired RNA replication resulting from reduced NS5A hyperphosphorylation has also been reported in the case of JFH-1 or JFH-1-based recombinant virus (25, 58–60). Consistent with a previous report (27), we found that CKI-α depletion inhibited the replication of the genotype 1b subgenomic replicon LucNeo#2, which carries the adaptive S2204R mutation in NS5A (38, 39) (Fig. 4C). Our transient-replication assay with the JFH-1 subgenomic replicon showed a slight but significant reduction in replication following CKI-α depletion (Fig. 4B). However, CKI-α silencing did not affect RNA replication in SGR-JFH1/LucNeo cells, where the JFH-1 subgenomic replicon stably replicates (Fig. 4C). Thus, the involvement of CKI-α in HCV RNA replication might be genotype or isolate dependent. We observed a difference in the replication capacity following CKI-α knockdown between transient and stable replication of JFH-1 replicons (Fig. 4B and C). A moderate reduction of replication was also detected when the JFH-1 genome carrying the S225A or S232A mutation was transiently transfected (Fig. 7B). One may infer that CKI-α is involved in the initiation of viral RNA replication rather than in its maintenance.

Our intra- and extracellular infectivity assays following CKI-α depletion suggested that CKI-α primarily targets virion assembly in the HCV life cycle (Fig. 4D to F), although a slight but nonnegligible negative effect of CKI-α knockdown on viral replication was observed (Fig. 4B). It is accepted that the assembly of HCV particles requires recruitment of NS proteins, including NS5A as well as structural proteins, to cytoplasmic membrane structures around LDs, leading to an interaction between NS5A and the core, which is important for efficient encapsidation of the viral genome (7, 8, 56). To understand how CKI-α is involved in virion assembly, we performed a subcellular fractionation assay and immunofluorescence confocal microscopy. Our subcellular fractionation assay clearly showed that hyperphosphorylated NS5A, p58, is mainly localized in low-density membrane fractions, while hypophosphorylated NS5A, p56, prefers high-density fractions. NS5A abundance in lighter fractions was decreased following CKI-α depletion (Fig. 5A). These results are supported by microscopic analyses that demonstrated that CKI-α silencing reduced colocalization of NS5A with LDs and the core (Fig. 5D and E). We tried to confirm the interaction of NS5A and core in HCVcc-infected cells that had been transfected with CKI-α siRNA or irrelevant siRNA. However, the interaction was not observed under this condition, presumably because immunoprecipitated NS5A and/or core was not abundant enough to assess their coimmunoprecipitation in siRNA-transfected cells. Alternatively, we assessed the interaction in Huh-7 cells coexpressing core and NS5A, although no p58 form (no functional NS5A) was detected in this setting. We clearly detected the interaction of NS5A and core in this experiment and found that CKI-α depletion had no significant effect on this interaction (data not shown). Taken together with the results of confocal microscopy (Fig. 5E), this finding might suggest that both (i) phosphorylation of serine residues in the C terminus of NS5A, which is involved in the generation of basally phosphorylated NS5A, as shown previously (8), and (ii) CKI-α-mediated hyperphosphorylation, in which serine residues in the LCS I region are mainly involved, are important for an efficient interaction between NS5A and core in HCV replicating cells. Collectively, CKI-α-mediated hyperphosphorylation of NS5A may contribute to an increase in the local concentration of NS5A at low-density membrane structures around LDs rather than in facilitating the physical interaction of NS5A and core. The relationship between the phosphorylation status of NS5A and its localization on cellular membranes has been previously reported. Miyanari et al. showed that mutated NS5A expressed from JFH-1 variants (JFH1^{AAA99} and JFH1^{AAA102} in their report), whose p58/p56 ratios were lower than that of wild-type virus, was not recruited to LDs (56). Qiu et al. fractionated lysates from replicon cells and demonstrated that a substantial amount of hyperphosphorylated NS5A was detected in lighter fractions. Treatment with an NS5A inhibitor, BMS-790052, reduced hyperphosphorylation of NS5A and concomitantly decreased the overall amount of NS5A in low-density membrane fractions (62). These findings raise questions about the regulatory mechanism(s) of the subcellular localization of NS5A, especially at low-density membrane structures. The above-mentioned NS5A mutants, JFH1^{AAA99} and JFH1^{AAA102}, have triple alanine substitutions for the APK sequence at aa 99 to 101 and the PPT sequence at aa 102 to 104 in NS5A, respectively, but neither is likely to be a CKI recognition site. In addition, the NS5A inhibitor

has no inhibitory effect on CKI activity (62). Thus, it appears that two or more kinds of serine/threonine-specific protein kinases, including CKI-α, participate in NS5A phosphorylation that is important for the regulation of its subcellular distribution. It is tempting to speculate that host factors involved in membrane trafficking or lipogenesis possibly interact with NS5A in a phosphorylation-dependent manner and facilitate recruitment of NS5A to low-density membrane structures surrounding LDs. Although further study is needed to validate this speculation, NS5A-interacting factors, such as VAP-A and diacylglycerol acyltransferase-1 (19, 63, 64), might be candidates for involvement in the regulation of this process.

To identify potential phospho-acceptor sites for CKI-α, a phospho-proteome analysis was carried out with NS5A isolated from HCVcc-infected cell lines with and without CKI-α knockdown (Fig. 6). Three kinds of phosphopeptides were identified out of a total of 629 peptides after peptide selection, although fine mapping of the phosphorylation sites was not completely successful. Among them, only the relative frequency of phosphopeptide 1 (GSPPSEASSSVSQLSAPSLR) was decreased after CKI-α knockdown, suggesting the possibility that peptide 1 contains amino acids phosphorylated by CKI-α. Serine residues in peptide 1, which are well conserved among HCV genotypes, matched the consensus sequences for CKI-α-mediated phosphorylation (57). In contrast, a threonine residue in peptide 2 is not conserved and does not match the consensus sequences for phosphorylation by CKI-α. The frequency of phosphopeptide 3 was unchanged with and without CKI-α knockdown (0.1% versus 0.1%). Further mutagenesis analyses targeting the peptide 1 region suggested that S225 and S232 are possible CKI-α phosphorylation sites involved in NS5A hyperphosphorylation and infectious virus production, because alanine substitution for either of these serine residues reproduced the viral phenotype after CKI-α knockdown more accurately than the other mutants within the peptide 1 region (Fig. 7B to E). The S229A and S235A mutations severely impaired viral replication, suggesting that phosphorylation at S229 and S235 is essential for efficient viral replication (Fig. 7B). However, the HCV protein expression assay using vaccinia virus expressing the T7 RNA polymerase revealed that phosphorylation of these residues is not involved in NS5A hyperphosphorylation (Fig. 7E). In the case of genotype 1 isolates, NS5A mutations that reduce hyperphosphorylation enhanced viral RNA replication (17, 18). However, this was not the case for the S225A or S232A mutation in genotype 2a. In addition, S229A and S235A mutations in genotype 1b (Con1) markedly enhance viral replication (18), but the same mutations are lethal in genotype 2a. S232 has been shown to be a potential phosphorylation site for CKI-α by a peptide-based kinase assay *in vitro* (28). However, the present study is the first to demonstrate the significance of phosphorylation at S225 and S232 in infectious virus production. The sequence coverage of NS5A by our mass spectrometry analysis was less than 60% and was especially low in domain III of NS5A (Fig. 6B). We cannot exclude the possibility of the presence of additional CKI-α phosphorylation sites in NS5A.

Recently, two cellular kinases involved in the regulation of NS5A phosphorylation have been identified. PI4K-IIIα is essential for HCV replication (65–70) and catalyzes the synthesis of phosphatidylinositol 4-phosphate accumulating in HCV replicating cells through its enzymatic activation resulting from an interaction with NS5A (71, 72). PI4K-IIIα directly interacts with the C-terminal end of NS5A domain I, and NS5A–PI4K-IIIα binding is essential for viral replication. Its depletion resulted in a relative increase of p58 abundance, while overexpression of enzymatically active PI4K-IIIα increased the relative abundance of p56 (73). Plk1 has been shown to play a role in viral replication through hyperphosphorylation of NS5A (25). Plk1 was coimmunoprecipitated with NS5A, and knockdown of Plk1 or treatment with a specific inhibitor decreased both NS5A hyperphosphorylation and HCV replication. Since the recognition sites for CKI-α, PI4K-IIIα, and Plk1 have been assumed to be spatially close to each other (25, 28, 73), it is interesting to analyze their interactive actions in regard to regulation of NS5A phosphorylation.

The exquisite balance between the two different phosphorylated forms of NS5A has been proposed to regulate the HCV life cycle; basally phosphorylated p56 abundance is hypothetically involved in viral RNA replication, and hyperphosphorylated p58 is required for virion assembly (9, 17, 18, 73, 74). However, this hypothesis has not yet been fully proven. Our results here provide strong evidence supporting the involvement of NS5A hyperphosphorylation in viral assembly and that of CKI-α in mediating this process. These results not only contribute to a better understanding of the regulatory details of the HCV life cycle but also illuminate targets for potential antiviral strategies.

ACKNOWLEDGMENTS

We are grateful to F. V. Chisari for kindly providing Huh7.5.1 cells, C. M. Rice for providing anti-NS5A mouse monoclonal antibody (9E10), K. Watashi and K. Shimotohno for providing LucNeo#2 cells, T. Pietschmann for providing the expression plasmid carrying the JFH-1 envelope glycoprotein gene, and Y. Matsuura for providing the plasmid expressing the VSV-G envelope glycoprotein. We thank D. Akazawa for help in preparing HCVpp, the Michael Hooker Microscopy Facility of the University of North Carolina for assistance with confocal microscopy, M. Sasaki, N. Sugiyama, K. Goto, and T. Date for their technical assistance, and T. Mizoguchi for secretarial assistance.

This work was supported in part by grants-in-aid from the Ministry of Health, Labor, and Welfare of Japan and the Ministry of Education, Culture, Sports, Science, and Technology, Japan, by Research on Health Sciences Focusing on Drug Innovation from the Japan Health Sciences Foundation, and by a grant (R01-AI095690) from the U.S. National Institutes of Health.

REFERENCES

1. **Shepard CW, Finelli L, Alter MJ.** 2005. Global epidemiology of hepatitis C virus infection. Lancet Infect. Dis. 5:558–567. http://dx.doi.org/10.1016/S1473-3099(05)70216-4.
2. **Alter MJ.** 2007. Epidemiology of hepatitis C virus infection. World J. Gastroenterol. 13:2436–2441. http://www.wjgnet.com/1007-9327/13/2436.asp.
3. **Choo QL, Richman KH, Han JH, Berger K, Lee C, Dong C, Gallegos C, Coit D, Medina-Selby R, Barr PJ, Weiner AJ, Bradley DW, Kuo G, Houghton M.** 1991. Genetic organization and diversity of the hepatitis C virus. Proc. Natl. Acad. Sci. U. S. A. 88:2451–2455. http://dx.doi.org/10.1073/pnas.88.6.2451.
4. **Suzuki T, Ishii K, Aizaki H, Wakita T.** 2007. Hepatitis C viral life cycle. Adv. Drug Deliv. Rev. 59:1200–1212. http://dx.doi.org/10.1016/j.addr.2007.04.014.
5. **Lohmann V, Korner F, Koch J, Herian U, Theilmann L, Bartenschlager R.** 1999. Replication of subgenomic hepatitis C virus RNAs in a hepatoma cell line. Science 285:110–113. http://dx.doi.org/10.1126/science.285.5424.110.
6. **Egger D, Wolk B, Gosert R, Bianchi L, Blum HE, Moradpour D, Bienz K.** 2002. Expression of hepatitis C virus proteins induces distinct membrane alterations including a candidate viral replication complex. J. Virol. 76:5974–5984. http://dx.doi.org/10.1128/JVI.76.12.5974-5984.2002.

7. Appel N, Zayas M, Miller S, Krijnse-Locker J, Schaller T, Friebe P, Kallis S, Engel U, Bartenschlager R. 2008. Essential role of domain III of nonstructural protein 5A for hepatitis C virus infectious particle assembly. PLoS Pathog. 4:e1000035. http://dx.doi.org/10.1371/journal.ppat.1000035.
8. Masaki T, Suzuki R, Murakami K, Aizaki H, Ishii K, Murayama A, Date T, Matsuura Y, Miyamura T, Wakita T, Suzuki T. 2008. Interaction of hepatitis C virus nonstructural protein 5A with core protein is critical for the production of infectious virus particles. J. Virol. 82:7964–7976. http://dx.doi.org/10.1128/JVI.00826-08.
9. Tellinghuisen TL, Foss KL, Treadaway J. 2008. Regulation of hepatitis C virion production via phosphorylation of the NS5A protein. PLoS Pathog. 4:e1000032. http://dx.doi.org/10.1371/journal.ppat.1000032.
10. Shi ST, Lee KJ, Aizaki H, Hwang SB, Lai MM. 2003. Hepatitis C virus RNA replication occurs on a detergent-resistant membrane that cofractionates with caveolin-2. J. Virol. 77:4160–4168. http://dx.doi.org/10.1128/JVI.77.7.4160-4168.2003.
11. Miyanari Y, Hijikata M, Yamaji M, Hosaka M, Takahashi H, Shimotohno K. 2003. Hepatitis C virus non-structural proteins in the probable membranous compartment function in viral genome replication. J. Biol. Chem. 278:50301–50308. http://dx.doi.org/10.1074/jbc.M305684200.
12. Tellinghuisen TL, Marcotrigiano J, Rice CM. 2005. Structure of the zinc-binding domain of an essential component of the hepatitis C virus replicase. Nature 435:374–379. http://dx.doi.org/10.1038/nature03580.
13. Huang L, Hwang J, Sharma SD, Hargittai MR, Chen Y, Arnold JJ, Raney KD, Cameron CE. 2005. Hepatitis C virus nonstructural protein 5A (NS5A) is an RNA-binding protein. J. Biol. Chem. 280:36417–36428. http://dx.doi.org/10.1074/jbc.M508175200.
14. Reed KE, Xu J, Rice CM. 1997. Phosphorylation of the hepatitis C virus NS5A protein in vitro and in vivo: properties of the NS5A-associated kinase. J. Virol. 71:7187–7197.
15. Tanji Y, Kaneko T, Satoh S, Shimotohno K. 1995. Phosphorylation of hepatitis C virus-encoded nonstructural protein NS5A. J. Virol. 69:3980–3986.
16. Kaneko T, Tanji Y, Satoh S, Hijikata M, Asabe S, Kimura K, Shimotohno K. 1994. Production of two phosphoproteins from the NS5A region of the hepatitis C viral genome. Biochem. Biophys. Res. Commun. 205:320–326. http://dx.doi.org/10.1006/bbrc.1994.2667.
17. Blight KJ, Kolykhalov AA, Rice CM. 2000. Efficient initiation of HCV RNA replication in cell culture. Science 290:1972–1974. http://dx.doi.org/10.1126/science.290.5498.1972.
18. Appel N, Pietschmann T, Bartenschlager R. 2005. Mutational analysis of hepatitis C virus nonstructural protein 5A: potential role of differential phosphorylation in RNA replication and identification of a genetically flexible domain. J. Virol. 79:3187–3194. http://dx.doi.org/10.1128/JVI.79.5.3187-3194.2005.
19. Evans MJ, Rice CM, Goff SP. 2004. Phosphorylation of hepatitis C virus nonstructural protein 5A modulates its protein interactions and viral RNA replication. Proc. Natl. Acad. Sci. U. S. A. 101:13038–13043. http://dx.doi.org/10.1073/pnas.0405152101.
20. Katze MG, Kwieciszewski B, Goodlett DR, Blakely CM, Neddermann P, Tan SL, Aebersold R. 2000. Ser(2194) is a highly conserved major phosphorylation site of the hepatitis C virus nonstructural protein NS5A. Virology 278:501–513. http://dx.doi.org/10.1006/viro.2000.0662.
21. Reed KE, Rice CM. 1999. Identification of the major phosphorylation site of the hepatitis C virus H strain NS5A protein as serine 2321. J. Biol. Chem. 274:28011–28018.
22. Nordle Gilliver A, Griffin S, Harris M. 2010. Identification of a novel phosphorylation site in hepatitis C virus NS5A. J. Gen. Virol. 91:2428–2432. http://dx.doi.org/10.1099/vir.0.023614-0.
23. Lemay KL, Treadaway J, Angulo I, Tellinghuisen TL. 2013. A hepatitis C virus NS5A phosphorylation site that regulates RNA replication. J. Virol. 87:1255–1260. http://dx.doi.org/10.1128/JVI.02154-12.
24. Neddermann P, Quintavalle M, Di Pietro C, Clementi A, Cerretani M, Altamura S, Bartholomew L, De Francesco R. 2004. Reduction of hepatitis C virus NS5A hyperphosphorylation by selective inhibition of cellular kinases activates viral RNA replication in cell culture. J. Virol. 78:13306–13314. http://dx.doi.org/10.1128/JVI.78.23.13306-13314.2004.
25. Chen YC, Su WC, Huang JY, Chao TC, Jeng KS, Machida K, Lai MM. 2010. Polo-like kinase 1 is involved in hepatitis C virus replication by hyperphosphorylating NS5A. J. Virol. 84:7983–7993. http://dx.doi.org/10.1128/JVI.00068-10.
26. Coito C, Diamond DL, Neddermann P, Korth MJ, Katze MG. 2004. High-throughput screening of the yeast kinome: identification of human serine/threonine protein kinases that phosphorylate the hepatitis C virus NS5A protein. J. Virol. 78:3502–3513. http://dx.doi.org/10.1128/JVI.78.7.3502-3513.2004.
27. Quintavalle M, Sambucini S, Di Pietro C, De Francesco R, Neddermann P. 2006. The alpha isoform of protein kinase CKI is responsible for hepatitis C virus NS5A hyperphosphorylation. J. Virol. 80:11305–11312. http://dx.doi.org/10.1128/JVI.01465-06.
28. Quintavalle M, Sambucini S, Summa V, Orsatti L, Talamo F, De Francesco R, Neddermann P. 2007. Hepatitis C virus NS5A is a direct substrate of casein kinase I-alpha, a cellular kinase identified by inhibitor affinity chromatography using specific NS5A hyperphosphorylation inhibitors. J. Biol. Chem. 282:5536–5544. http://dx.doi.org/10.1074/jbc.M610486200.
29. Kato T, Date T, Miyamoto M, Sugiyama M, Tanaka Y, Orito E, Ohno T, Sugihara K, Hasegawa I, Fujiwara K, Ito K, Ozasa A, Mizokami M, Wakita T. 2005. Detection of anti-hepatitis C virus effects of interferon and ribavirin by a sensitive replicon system. J. Clin. Microbiol. 43:5679–5684. http://dx.doi.org/10.1128/JCM.43.11.5679-5684.2005.
30. Wakita T, Pietschmann T, Kato T, Date T, Miyamoto M, Zhao Z, Murthy K, Habermann A, Krausslich HG, Mizokami M, Bartenschlager R, Liang TJ. 2005. Production of infectious hepatitis C virus in tissue culture from a cloned viral genome. Nat. Med. 11:791–796. http://dx.doi.org/10.1038/nm1268.
31. Phan T, Beran RK, Peters C, Lorenz IC, Lindenbach BD. 2009. Hepatitis C virus NS2 protein contributes to virus particle assembly via opposing epistatic interactions with the E1–E2 glycoprotein and NS3-NS4A enzyme complexes. J. Virol. 83:8379–8395. http://dx.doi.org/10.1128/JVI.00891-09.
32. Tannous BA, Kim DE, Fernandez JL, Weissleder R, Breakefield XO. 2005. Codon-optimized Gaussia luciferase cDNA for mammalian gene expression in culture and in vivo. Mol. Ther. 11:435–443. http://dx.doi.org/10.1016/j.ymthe.2004.10.016.
33. Ryan MD, King AM, Thomas GP. 1991. Cleavage of foot-and-mouth disease virus polyprotein is mediated by residues located within a 19 amino acid sequence. J. Gen. Virol. 72:2727–2732. http://dx.doi.org/10.1099/0022-1317-72-11-2727.
34. Niwa H, Yamamura K, Miyazaki J. 1991. Efficient selection for high-expression transfectants with a novel eukaryotic vector. Gene 108:193–199. http://dx.doi.org/10.1016/0378-1119(91)90434-D.
35. Zhong J, Gastaminza P, Cheng G, Kapadia S, Kato T, Burton DR, Wieland SF, Uprichard SL, Wakita T, Chisari FV. 2005. Robust hepatitis C virus infection in vitro. Proc. Natl. Acad. Sci. U. S. A. 102:9294–9299. http://dx.doi.org/10.1073/pnas.0503596102.
36. Akazawa D, Date T, Morikawa K, Murayama A, Miyamoto M, Kaga M, Barth H, Baumert TF, Dubuisson J, Wakita T. 2007. CD81 expression is important for the permissiveness of Huh7 cell clones for heterogeneous hepatitis C virus infection. J. Virol. 81:5036–5045. http://dx.doi.org/10.1128/JVI.01573-06.
37. Kato T, Date T, Miyamoto M, Furusaka A, Tokushige K, Mizokami M, Wakita T. 2003. Efficient replication of the genotype 2a hepatitis C virus subgenomic replicon. Gastroenterology 125:1808–1817. http://dx.doi.org/10.1053/j.gastro.2003.09.023.
38. Murata T, Ohshima T, Yamaji M, Hosaka M, Miyanari Y, Hijikata M, Shimotohno K. 2005. Suppression of hepatitis C virus replicon by TGF-beta. Virology 331:407–417. http://dx.doi.org/10.1016/j.virol.2004.10.036.
39. Goto K, Watashi K, Murata T, Hishiki T, Hijikata M, Shimotohno K. 2006. Evaluation of the anti-hepatitis C virus effects of cyclophilin inhibitors, cyclosporin A, and NIM811. Biochem. Biophys. Res. Commun. 343:879–884. http://dx.doi.org/10.1016/j.bbrc.2006.03.059.
40. Murayama A, Sugiyama N, Yoshimura S, Ishihara-Sugano M, Masaki T, Kim S, Wakita T, Mishiro S, Kato T. 2012. A subclone of HuH-7 with enhanced intracellular hepatitis C virus production and evasion of virus related-cell cycle arrest. PLoS One 7:e52697. http://dx.doi.org/10.1371/journal.pone.0052697.
41. Tadokoro D, Takahama S, Shimizu K, Hayashi S, Endo Y, Sawasaki T. 2010. Characterization of a caspase-3-substrate kinome using an N- and C-terminally tagged protein kinase library produced by a cell-free system. Cell Death Dis. 1:e89. http://dx.doi.org/10.1038/cddis.2010.65.
42. Sawasaki T, Gouda MD, Kawasaki T, Tsuboi T, Tozawa Y, Takai K, Endo Y. 2005. The wheat germ cell-free expression system: methods for high-throughput materialization of genetic information. Methods Mol. Biol. 310:131–144. http://dx.doi.org/10.1007/978-1-59259-948-6_10.
43. Sawasaki T, Ogasawara T, Morishita R, Endo Y. 2002. A cell-free protein

synthesis system for high-throughput proteomics. Proc. Natl. Acad. Sci. U. S. A. 99:14652–14657. http://dx.doi.org/10.1073/pnas.232580399.
44. Sawasaki T, Kamura N, Matsunaga S, Saeki M, Tsuchimochi M, Morishita R, Endo Y. 2008. Arabidopsis HY5 protein functions as a DNA-binding tag for purification and functional immobilization of proteins on agarose/DNA microplate. FEBS Lett. 582:221–228. http://dx.doi.org/10.1016/j.febslet.2007.12.004.
45. Bartosch B, Dubuisson J, Cosset FL. 2003. Infectious hepatitis C virus pseudo-particles containing functional E1–E2 envelope protein complexes. J. Exp. Med. 197:633–642. http://dx.doi.org/10.1084/jem.20021756.
46. Masaki T, Suzuki R, Saeed M, Mori K, Matsuda M, Aizaki H, Ishii K, Maki N, Miyamura T, Matsuura Y, Wakita T, Suzuki T. 2010. Production of infectious hepatitis C virus by using RNA polymerase I-mediated transcription. J. Virol. 84:5824–5835. http://dx.doi.org/10.1128/JVI.02397-09.
47. Masaki T, Matsuura T, Ohkawa K, Miyamura T, Okazaki I, Watanabe T, Suzuki T. 2006. All-trans retinoic acid down-regulates human albumin gene expression through the induction of C/EBPβ-LIP. Biochem. J. 397:345–353. http://dx.doi.org/10.1042/BJ20051863.
48. Iwahori T, Matsuura T, Maehashi H, Sugo K, Saito M, Hosokawa M, Chiba K, Masaki T, Aizaki H, Ohkawa K, Suzuki T. 2003. CYP3A4 inducible model for in vitro analysis of human drug metabolism using a bioartificial liver. Hepatology 37:665–673. http://dx.doi.org/10.1053/jhep.2003.50094.
49. Li Q, Lau A, Morris TJ, Guo L, Fordyce CB, Stanley EF. 2004. A syntaxin 1, Gα(o), and N-type calcium channel complex at a presynaptic nerve terminal: analysis by quantitative immunocolocalization. J. Neurosci. 24:4070–4081. http://dx.doi.org/10.1523/JNEUROSCI.0346-04.2004.
50. Kim J, Lee D, Choe J. 1999. Hepatitis C virus NS5A protein is phosphorylated by casein kinase II. Biochem. Biophys. Res. Commun. 257:777–781. http://dx.doi.org/10.1006/bbrc.1999.0460.
51. Ide Y, Tanimoto A, Sasaguri Y, Padmanabhan R. 1997. Hepatitis C virus NS5A protein is phosphorylated in vitro by a stably bound protein kinase from HeLa cells and by cAMP-dependent protein kinase A-alpha catalytic subunit. Gene 201:151–158. http://dx.doi.org/10.1016/S0378-1119(97)00440-X.
52. Benga WJ, Krieger SE, Dimitrova M, Zeisel MB, Parnot M, Lupberger J, Hildt E, Luo G, McLauchlan J, Baumert TF, Schuster C. 2010. Apolipoprotein E interacts with hepatitis C virus nonstructural protein 5A and determines assembly of infectious particles. Hepatology 51:43–53. http://dx.doi.org/10.1002/hep.23278.
53. Farquhar MJ, Harris HJ, Diskar M, Jones S, Mee CJ, Nielsen SU, Brimacombe CL, Molina S, Toms GL, Maurel P, Howl J, Herberg FW, van Ijzendoorn SC, Balfe P, McKeating JA. 2008. Protein kinase A-dependent step(s) in hepatitis C virus entry and infectivity. J. Virol. 82:8797–8811. http://dx.doi.org/10.1128/JVI.00592-08.
54. Evans MJ, von Hahn T, Tscherne DM, Syder AJ, Panis M, Wolk B, Hatziioannou T, McKeating JA, Bieniasz PD, Rice CM. 2007. Claudin-1 is a hepatitis C virus co-receptor required for a late step in entry. Nature 446:801–805. http://dx.doi.org/10.1038/nature05654.
55. Matsumura T, Kato T, Sugiyama N, Tasaka-Fujita M, Murayama A, Masaki T, Wakita T, Imawari M. 2012. 25-Hydroxyvitamin D3 suppresses hepatitis C virus production. Hepatology 56:1231–1239. http://dx.doi.org/10.1002/hep.25763.
56. Miyanari Y, Atsuzawa K, Usuda N, Watashi K, Hishiki T, Zayas M, Bartenschlager R, Wakita T, Hijikata M, Shimotohno K. 2007. The lipid droplet is an important organelle for hepatitis C virus production. Nat. Cell Biol. 9:1089–1097. http://dx.doi.org/10.1038/ncb1631.
57. Ubersax JA, Ferrell JE, Jr. 2007. Mechanisms of specificity in protein phosphorylation. Nat. Rev. Mol. Cell Biol. 8:530–541. http://dx.doi.org/10.1038/nrm2203.
58. Ross-Thriepland D, Harris M. 2014. Insights into the complexity and functionality of hepatitis C virus NS5A phosphorylation. J. Virol. 88:1421–1432. http://dx.doi.org/10.1128/JVI.03017-13.
59. Fridell RA, Valera L, Qiu D, Kirk MJ, Wang C, Gao M. 2013. Intragenic complementation of hepatitis C virus NS5A RNA replication-defective alleles. J. Virol. 87:2320–2329. http://dx.doi.org/10.1128/JVI.02861-12.
60. Fridell RA, Qiu D, Valera L, Wang C, Rose RE, Gao M. 2011. Distinct functions of NS5A in hepatitis C virus RNA replication uncovered by studies with the NS5A inhibitor BMS-790052. J. Virol. 85:7312–7320. http://dx.doi.org/10.1128/JVI.00253-11.
61. Kim S, Welsch C, Yi M, Lemon SM. 2011. Regulation of the production of infectious genotype 1a hepatitis C virus by NS5A domain III. J. Virol. 85:6645–6656. http://dx.doi.org/10.1128/JVI.02156-10.
62. Qiu D, Lemm JA, O'Boyle DR, II, Sun JH, Nower PT, Nguyen V, Hamann LG, Snyder LB, Deon DH, Ruediger E, Meanwell NA, Belema M, Gao M, Fridell RA. 2011. The effects of NS5A inhibitors on NS5A phosphorylation, polyprotein processing and localization. J. Gen. Virol. 92:2502–2511. http://dx.doi.org/10.1099/vir.0.034801-0.
63. Camus G, Herker E, Modi AA, Haas JT, Ramage HR, Farese RV, Jr, Ott M. 2013. Diacylglycerol acyltransferase-1 localizes hepatitis C virus NS5A protein to lipid droplets and enhances NS5A interaction with the viral capsid core. J. Biol. Chem. 288:9915–9923. http://dx.doi.org/10.1074/jbc.M112.434910.
64. Gao L, Aizaki H, He JW, Lai MM. 2004. Interactions between viral nonstructural proteins and host protein hVAP-33 mediate the formation of hepatitis C virus RNA replication complex on lipid raft. J. Virol. 78:3480–3488. http://dx.doi.org/10.1128/JVI.78.7.3480-3488.2004.
65. Berger KL, Cooper JD, Heaton NS, Yoon R, Oakland TE, Jordan TX, Mateu G, Grakoui A, Randall G. 2009. Roles for endocytic trafficking and phosphatidylinositol 4-kinase III alpha in hepatitis C virus replication. Proc. Natl. Acad. Sci. U. S. A. 106:7577–7582. http://dx.doi.org/10.1073/pnas.0902693106.
66. Vaillancourt FH, Pilote L, Cartier M, Lippens J, Liuzzi M, Bethell RC, Cordingley MG, Kukolj G. 2009. Identification of a lipid kinase as a host factor involved in hepatitis C virus RNA replication. Virology 387:5–10. http://dx.doi.org/10.1016/j.virol.2009.02.039.
67. Borawski J, Troke P, Puyang X, Gibaja V, Zhao S, Mickanin C, Leighton-Davies J, Wilson CJ, Myer V, Cornellataracido I, Baryza J, Tallarico J, Joberty G, Bantscheff M, Schirle M, Bouwmeester T, Mathy JE, Lin K, Compton T, Labow M, Wiedmann B, Gaither LA. 2009. Class III phosphatidylinositol 4-kinase alpha and beta are novel host factor regulators of hepatitis C virus replication. J. Virol. 83:10058–10074. http://dx.doi.org/10.1128/JVI.02418-08.
68. Tai AW, Benita Y, Peng LF, Kim SS, Sakamoto N, Xavier RJ, Chung RT. 2009. A functional genomic screen identifies cellular cofactors of hepatitis C virus replication. Cell Host. Microbe 5:298–307. http://dx.doi.org/10.1016/j.chom.2009.02.001.
69. Li Q, Brass AL, Ng A, Hu Z, Xavier RJ, Liang TJ, Elledge SJ. 2009. A genome-wide genetic screen for host factors required for hepatitis C virus propagation. Proc. Natl. Acad. Sci. U. S. A. 106:16410–16415. http://dx.doi.org/10.1073/pnas.0907439106.
70. Trotard M, Lepere-Douard C, Regeard M, Piquet-Pellorce C, Lavillette D, Cosset FL, Gripon P, Le Seyec J. 2009. Kinases required in hepatitis C virus entry and replication highlighted by small interference RNA screening. FASEB J. 23:3780–3789. http://dx.doi.org/10.1096/fj.09-131920.
71. Reiss S, Rebhan I, Backes P, Romero-Brey I, Erfle H, Matula P, Kaderali L, Poenisch M, Blankenburg H, Hiet MS, Longerich T, Diehl S, Ramirez F, Balla T, Rohr K, Kaul A, Buhler S, Pepperkok R, Lengauer T, Albrecht M, Eils R, Schirmacher P, Lohmann V, Bartenschlager R. 2011. Recruitment and activation of a lipid kinase by hepatitis C virus NS5A is essential for integrity of the membranous replication compartment. Cell Host Microbe 9:32–45. http://dx.doi.org/10.1016/j.chom.2010.12.002.
72. Berger KL, Kelly SM, Jordan TX, Tartell MA, Randall G. 2011. Hepatitis C virus stimulates the phosphatidylinositol 4-kinase III alpha-dependent phosphatidylinositol 4-phosphate production that is essential for its replication. J. Virol. 85:8870–8883. http://dx.doi.org/10.1128/JVI.00059-11.
73. Reiss S, Harak C, Romero-Brey I, Radujkovic D, Klein R, Ruggieri A, Rebhan I, Bartenschlager R, Lohmann V. 2013. The lipid kinase phosphatidylinositol-4 kinase III alpha regulates the phosphorylation status of hepatitis C virus NS5A. PLoS Pathog. 9:e1003359. http://dx.doi.org/10.1371/journal.ppat.1003359.
74. Pietschmann T, Zayas M, Meuleman P, Long G, Appel N, Koutsoudakis G, Kallis S, Leroux-Roels G, Lohmann V, Bartenschlager R. 2009. Production of infectious genotype 1b virus particles in cell culture and impairment by replication enhancing mutations. PLoS Pathog. 5:e1000475. http://dx.doi.org/10.1371/journal.ppat.1000475.

zjv00415/zjv0052d15z | xppws | S=1 | 12/10/14 | 12:17 | 4/C Fig: 10 | ArtID: 03385-14 | NLM: research-article | CE: sj

Editor: Perlman | Section: Virus-Cell Interactions | Designation: T

JVI Journals.ASM.org

Targeting Cellular Squalene Synthase, an Enzyme Essential for Cholesterol Biosynthesis, Is a Potential Antiviral Strategy against Hepatitis C Virus

AQ: au Kyoko Saito,[a] Yoshitaka Shirasago,[a,b] Tetsuro Suzuki,[c] Hideki Aizaki,[d] Kentaro Hanada,[a] Takaji Wakita,[d] Masahiro Nishijima,[e] Masayoshi Fukasawa[a]

AQ: aff Department of Biochemistry and Cell Biology, National Institute of Infectious Diseases, Tokyo, Japan[a]; Graduate School of Biological Science, Tokyo University of Science, Tokyo, Japan[b]; Department of Infectious Diseases, Hamamatsu University School of Medicine, Hamamatsu, Japan[c]; Department of Virology II, National Institute of Infectious Diseases, Tokyo, Japan[d]; Showa Pharmaceutical University, Machida, Japan[e]

ABSTRACT

Hepatitis C virus (HCV) exploits host membrane cholesterol and its metabolism for progeny virus production. Here, we examined the impact of targeting cellular squalene synthase (SQS), the first committed enzyme for cholesterol biosynthesis, on HCV production. By using the HCV JFH-1 strain and human hepatoma Huh-7.5.1-derived cells, we found that the SQS inhibitors YM-53601 and zaragozic acid A decreased viral RNA, protein, and progeny production in HCV-infected cells without affecting cell viability. Similarly, small interfering RNA (siRNA)-mediated knockdown of SQS led to significantly reduced HCV production, confirming the enzyme as an antiviral target. A metabolic labeling study demonstrated that YM-53601 suppressed the biosynthesis of cholesterol and cholesteryl esters at antiviral concentrations. Unlike YM-53601, the cholesterol esterification inhibitor Sandoz 58-035 did not exhibit an antiviral effect, suggesting that biosynthesis of cholesterol is more important than that of cholesteryl esters for HCV production. YM-53601 inhibited transient replication of a JFH-1 subgenomic replicon and entry of JFH-1 pseudoparticles, suggesting that at least suppression of viral RNA replication and entry contributes to the antiviral effect of the drug. Collectively, our findings highlight the importance of the cholesterol biosynthetic pathway in HCV production and implicate SQS as a potential target for antiviral strategies against HCV.

IMPORTANCE

Hepatitis C virus (HCV) is known to be closely associated with host cholesterol and its metabolism throughout the viral life cycle. However, the impact of targeting cholesterol biosynthetic enzymes on HCV production is not fully understood. We found that squalene synthase, the first committed enzyme for cholesterol biosynthesis, is important for HCV production, and we propose this enzyme as a potential anti-HCV target. We provide evidence that synthesis of free cholesterol is more important than that of esterified cholesterol for HCV production, highlighting a marked free cholesterol dependency of HCV production. Our findings also offer a new insight into a role of the intracellular cholesterol pool that is coupled to its biosynthesis in the HCV life cycle.

Hepatitis C virus (HCV) is a causative agent of acute and chronic hepatitis, which can eventually lead to cirrhosis and hepatocellular carcinoma. HCV infection is recognized as a major threat to global public health, with 130 to 150 million people worldwide being infected with the virus (1). Over the last decade, the standard therapy for chronic HCV infection has been a combination of pegylated interferon alpha and ribavirin (2), but that has greatly changed after the emergence of first direct-acting antivirals that selectively target HCV, i.e., telaprevir and boceprevir (3, 4). These drugs, both used in combination with pegylated interferon and ribavirin, have brought significant benefits to patients who did not respond to the conventional therapy. In addition, recent clinical data on the newly approved direct-acting antivirals simeprevir and sofosbuvir have provided novel insights on combination therapies with inhibitors of multiple targets (5). However, direct-acting antivirals are frequently associated with the emergence of drug-resistant HCV variants, likely leading to treatment failure (6). Thus, development of host-targeted agents, which are expected to have a high genetic barrier to resistance, should be encouraged to expand treatment options for chronic hepatitis C.

HCV is an enveloped, positive-sense, single-stranded RNA virus belonging to the *Hepacivirus* genus of the *Flaviviridae* family. The HCV genome is 9.6 kb in length and contains a single open reading frame encoding a large polyprotein of approximately 3,000 amino acids. Translation of the polyprotein is directed by an internal ribosome entry site (IRES) located mostly in the highly conserved 5′ untranslated region (7). The polyprotein is co- and posttranslationally processed into three structural proteins (core, E1, and E2), a small ion channel protein (p7), and six nonstructural proteins (NS2, NS3, NS4A, NS4B, NS5A, and NS5B) by cel-

Received 24 November 2014 Accepted 26 November 2014
Accepted manuscript posted online 3 December 2014
Citation Saito K, Shirasago Y, Suzuki T, Aizaki H, Hanada K, Wakita T, Nishijima M, Fukasawa M. 2015. Targeting cellular squalene synthase, an enzyme essential for cholesterol biosynthesis, is a potential antiviral strategy against hepatitis C virus. J Virol 89:000–000. doi:10.1128/JVI.03385-14.
Editor: S. Perlman
Address correspondence to Masayoshi Fukasawa, fuka@nih.go.jp.

doi:10.1128/JVI.03385-14

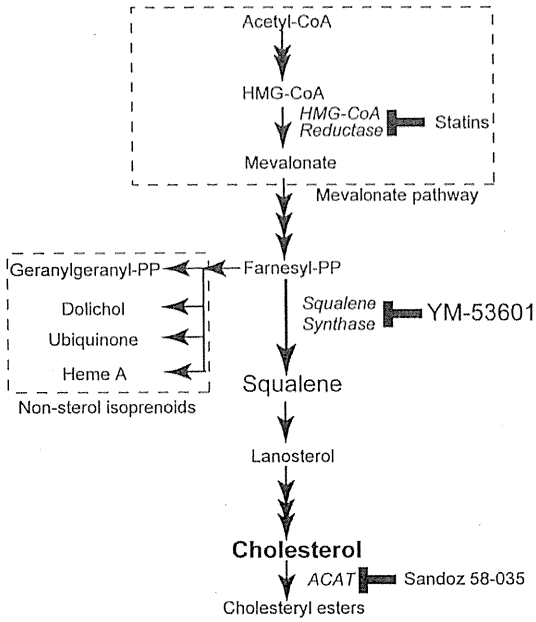

FIG 1 Cholesterol biosynthetic pathway in mammalian cells. Enzymes are shown in italics; inhibitors for the enzymes are shown next to the enzymes. Abbreviations: CoA, coenzyme A; HMG, 3-hydroxy-3-methylglutaryl; PP, pyrophosphate; ACAT, acyl-CoA:cholesterol acyltransferase.

lular and viral proteases (8–10). The nonstructural proteins assemble on the endoplasmic reticulum (ER)-derived membranes and recruit the viral genome into an RNA replication complex (11, 12).

Several lines of evidence suggest that HCV is closely associated with cholesterol and its metabolism throughout the viral life cycle in hepatocytes (13). In a previous study using a cholesterol-extracting drug, methyl-β-cyclodextrin, HCV entry was found to be in part dependent on the host membrane cholesterol content (14). Biochemical studies suggest that HCV RNA replication takes place on lipid rafts (15–17), i.e., detergent-resistant membrane microdomains enriched in cholesterol and sphingolipids (18). Lipid rafts also appear to be involved in HCV virion assembly because the viral structural proteins are associated with them (19, 20). Virion assembly occurs at the ER membranes immediately adjacent to the lipid droplet (21, 22), a major storage organelle for cholesteryl esters and triglycerides. Subsequent maturation and release of viral particles are tightly linked to the very-low-density lipoprotein (VLDL) secretion pathway (reference 22 and references therein; 23). Indeed, the lipid composition of secreted viral particles resembles that of VLDLs and low-density lipoproteins (LDLs), with a large amount of cholesteryl esters (24). The viral particles are also enriched in cholesterol and sphingomyelin, both of which are important for particle maturation and infectivity (19).

Cholesterol is synthesized from acetyl coenzyme A (acetyl-CoA) via a series of enzymatic reactions shown in Fig. 1. The rate-limiting enzyme of the cholesterol biosynthetic pathway is 3-hydroxy-3-methylglutaryl (HMG)-CoA reductase, which catalyzes the synthesis of mevalonate (25). Previous studies have shown that HMG-CoA reductase inhibitors or statins (26) block viral RNA replication in HCV genotype 1b replicon cells (27–29). Although statins are widely used as cholesterol-lowering drugs (30), their anti-HCV effect has been attributed not to a decrease in cholesterol content but rather to decreases of the nonsterol isoprenoids geranylgeranyl lipids (27, 28), the biosynthetic pathway of which shares early steps with that of cholesterol (Fig. 1). Although recent studies have shown that downstream enzymes in the cholesterol biosynthetic pathway, such as oxidosqualene cyclase, lanosterol C_{14}-demethylase, 24-dehydrocholesterol reductase, and 7-dehydrocholesterol reductase, are required for HCV production (31–33), the role of the committed steps of cholesterol biosynthesis in the HCV life cycle is not fully understood.

In this study, we focused on squalene synthase (SQS), which is the first committed enzyme in cholesterol biosynthesis (34) (Fig. 1). We examined the impact of SQS inhibition on HCV production by using an HCV cell culture system with human hepatoma Huh-7.5.1-derived cells and an HCV genotype 2a isolate, JFH-1 (35–37). We present data showing that SQS-mediated cholesterol biosynthesis is important for viral production, and we propose that SQS is a potential anti-HCV target.

MATERIALS AND METHODS

Reagents. YM-53601 (38), zaragozic acid A (39), and Sandoz 58-035 (40) were purchased from Sigma-Aldrich Corp. (St. Louis, MO, USA) and dissolved in dimethyl sulfoxide (DMSO). A Stealth RNA interference (RNAi) small interfering RNA (siRNA) for human SQS, HSS103617 (siSQS), and a Stealth RNAi negative-control low-GC duplex (siCONT) were purchased from Life Technologies Corp. (Carlsbad, CA, USA). Human low-density lipoprotein was purchased from Biomedical Technologies, Inc. (Stoughton, MA, USA). [*methyl*-^{3}H]acetate was purchased from Moravek Biochemicals, Inc. (Brea, CA, USA).

Cell culture. A highly HCV-permissive subclonal cell line derived from Huh-7.5.1 cells (36), Huh-7.5.1-8 (37), was maintained at 37°C and 5% CO_2 in Dulbecco's modified Eagle's medium that contained 10% fetal bovine serum, 0.1 mM nonessential amino acids, 100 units/ml penicillin G, and 100 μg/ml streptomycin sulfate (referred to as "complete medium"). Serum-free culture was performed as described previously (41) with slight modifications: Huh-7.5.1-8 cells were incubated at 37°C and 5% CO_2 in Dulbecco's modified Eagle's medium that contained 1% Nutridoma-SP (Roche Applied Science, Penzberg, Upper Bavaria, Germany) and 25 μg/ml gentamicin (referred to as "serum-free medium").

Virus stock and infection. HCV JFH-1 virus was prepared from culture supernatants of Huh-7.5.1-8 cells that had been transfected with *in vitro*-transcribed JFH-1 RNA as previously described (35). After serial passages of the JFH-1 virus in naive Huh-7.5.1-8 cells, infectious culture supernatants were collected and used as viral stocks in this study. Virus titers were determined by fluorescent-focus assays as previously described (42). For infection, cells were incubated with the virus at a multiplicity of infection of 4 fluorescent-focus-forming units/cell in complete medium for 2 h at 37°C.

Immunoblotting. Cells were lysed in NuPAGE lithium dodecyl sulfate (LDS) sample buffer (Life Technologies Corp.) that contained 0.05 M dithiothreitol (DTT) and then heated at 95°C for 5 min. The resultant lysates were subjected to SDS-polyacrylamide gel electrophoresis on NuPAGE 4 to 12% Bis-Tris gels (Life Technologies Corp.) and then transferred to Immun-Blot polyvinylidene difluoride membranes (Bio-Rad Laboratories, Inc., Hercules, CA, USA) according to the manufacturer's protocols. After being blocked with 5% (wt/vol) skim milk in TBS-T (0.05 M Tris-HCl [pH 7.6], 0.15 M NaCl, 0.1% [vol/vol] Tween 20), the membranes were probed with 1:5,000 dilutions of anti-HCV core monoclonal antibody (B2; Anogen, Yes Biotech Laboratories, Ltd., Mississauga, Ontario, Canada) or anti-HCV NS3 monoclonal antibody (8G-2; Abcam, Plc., Cambridge, United Kingdom) or with a 1:10,000 dilution of anti-glyceraldehyde-3-phosphate dehydrogenase (anti-GAPDH) monoclonal antibody (6C5; Abcam, Plc.), followed by a 1:5,000 dilution of horseradish

peroxidase-conjugated AffiniPure goat anti-mouse IgG(H+L) (Jackson ImmunoResearch Laboratories, Inc., West Grove, PA, USA) in TBS-T that contained 2% (wt/vol) skim milk. For detection of SQS, the membranes were probed with a 1:5,000 dilution of anti-SQS polyclonal antibody (B01; Abnova Corp., Taipei City, Taiwan) followed by a 1:5,000 dilution of horseradish peroxidase-conjugated AffiniPure goat anti-rabbit IgG(H+L) (Jackson ImmunoResearch Laboratories, Inc.). Each protein band complexed with the antibody on the membrane was visualized with an enhanced chemiluminescence immunoblotting detection system (GE Healthcare, UK Ltd., Little Chalfont, United Kingdom; Merck Millipore, Billerica, USA) and quantified using Image J 1.440 software (National Institutes of Health, Bethesda, MD, USA).

RT-qPCR analysis. Total RNA was isolated from cells by using an RNeasy Plus minikit (Qiagen, GmbH, Hilden, Germany) and reverse transcribed by random hexamer primers using a Transcriptor first-strand cDNA synthesis kit (Roche Applied Science) according to the manufacturer's protocols. Quantitative reverse transcription-PCR (RT-qPCR) was carried out on the LightCycler system (Roche Applied Science) using LightCycler FastStart DNA Master SYBR green I (Roche Applied Science) and specific primers for the core sequence (5′-CGCAACGTGGGTAAAG TCATCG-3′ and 5′-CGGGTAGGTTCCCTGTTGCATAA-3′), the NS5B sequence (5′-CAAGGGTCAAACCTGCGGTTACA-3′ and 5′-TGACTA CTAGGTCATCGCCGCATAC-3′), or the human GAPDH sequence (Search–LC, GmbH, Heidelberg, Germany). The relative amounts of viral RNA were calculated by dividing the copy number of a viral transcript by that of a GAPDH transcript in the same sample.

Metabolic labeling of lipids with radioactive acetate and TLC. Cells were plated at 1×10^5 cells per well of a 6-well plate 1 day before labeling and then incubated with [^{3}H]acetate (1.85 MBq/well) in serum-free medium for various periods. The cells were washed and harvested with phosphate-buffered saline (PBS), and a lipid fraction was extracted from the cells according to the method of Bligh and Dyer (43). The lipid fraction was spotted on a silica gel 60 plate (Merck Millipore) and separated by thin-layer chromatography (TLC) using hexane-diethyl ether-acetate (70:30:1, vol/vol/vol). The incorporation of ^{3}H radioactivity into each lipid was quantified using a BAS-1800 Bio-Image Analyzer (Fujifilm Corp.) or a Typhoon FLA 7000 biomolecular imager (GE Healthcare, UK Ltd.) and then normalized with the protein levels.

Determination of cholesterol and cholesteryl ester contents. Cells were disrupted in PBS by sonication. The lipid fraction was extracted from the cells as described above. The content of cholesterol in the lipid fraction was determined by an enzymatic colorimetric method using the Wako free cholesterol E test (Wako Pure Chemical Industries, Ltd., Osaka, Japan) according to the manufacturer's protocol and then normalized with the protein levels. The content of cholesteryl esters in the lipid fraction was determined by a direct measurement method for the enzymatic determination of cholesteryl esters as described elsewhere (44) and then normalized with the protein levels.

siRNA transfection. Cells were plated at 3×10^4 cells per well in 24-well plates 2 days before transfection and grown in complete medium. siRNA was complexed with Lipofectamine RNAiMAX transfection reagent (Life Technologies Corp.) according to the manufacturer's protocol and then added to the cells at a final concentration of 5 nM. After 5 h of incubation, the cells were washed and then placed in serum-free medium.

Subgenomic replicon plasmids. The HCV subgenomic replicon plasmids used in this study contain the T7 promoter followed by a bicistronic replicon sequence; the first is a part of the core region fused to either the luciferase (*luc*) gene of the firefly *Photinus pyralis* or the neomycin phosphotransferase (*neo*) gene translated under the control of the HCV IRES, and the second is the NS3-NS5B-coding region translated under the control of the encephalomyocarditis virus (EMCV) IRES. Subgenomic replicon plasmids of the JFH-1 strain, pSGR-JFH1/Luc and pSGR-JFH1/Luc-GND (45), carry the *luc* gene; the latter contains a GDD-to-GND mutation in NS5B, which abolishes RNA polymerase activity. Subgenomic replicon plasmids of the Con-1 strain (genotype 1b), pFK-I_{389}Luci/NS3-3′/NK5.1 and pFK-I_{389}neo/NS3-3′/NK5.1/ΔGDD (46), were kindly provided by Ralf Bartenschlager (University of Heidelberg, Germany) and carry the *luc* gene and the *neo* gene, respectively; the latter contains a deletion in the GDD active site of NS5B that abolishes RNA polymerase activity. A replication-incompetent mutant of pFK-I_{389}Luci/NS3-3′/NK5.1 was prepared by replacing an AscI-PmeI fragment that codes for the *neo* gene of pFK-I_{389}neo/NS3-3′/NK5.1/ΔGDD with the corresponding fragment that codes for the *luc* gene from pFK-I_{389}Luci/NS3-3′/NK5.1 (referred to as pFK-I_{389}/Luci/NS3-3′/NK5.1/ΔGDD).

***In vitro* transcription of RNA.** Linearization of plasmids, *in vitro* transcription with T7 RNA polymerase, and RNA purification were performed as previously described (47) except that the AmpliScribe T7 high-yield transcription kit (Epicentre Biotechnologies Corp., Madison, WI, USA) was used.

Transfection with *in vitro*-transcribed RNA. Electroporation was performed as described previously (48) with slight modifications. Cells (1×10^7 to 2×10^7) were mixed with 20 to 25 μg of *in vitro*-transcribed RNA in K-PBS (30 mM NaCl, 120 mM KCl, 8 mM Na_2HPO_4, 1.5 mM KH_2PO_4, and 5 mM $MgCl_2$, pH 7.9) and then pulsed at 975 μF and 290 V in a cuvette with a gap width of 0.4 cm by using a Gene Pulser Xcell system (Bio-Rad Laboratories, Inc.). For lipofection, cells were plated at 3×10^4 cells per well in a 24-well plate 2 days before transfection. The cells were then transfected with 0.5 μg of *in vitro*-transcribed RNA for 3 h using the TransMessenger transfection reagent (Qiagen, GmbH) according to the manufacturer's protocol.

Luciferase assay. Cells were lysed with cell culture lysis reagent (Promega Corp., Madison, WI, USA). Five microliters of the lysate was mixed with 25 μl of luciferase assay reagent (Promega Corp.), and then luciferase activity in the lysate was measured by using a Luminescencer-PSN luminometer (Atto Corp., Tokyo, Japan).

Preparation of HA-tagged NS4B-expressing cells. An expression plasmid that encodes NS4B protein N-terminally fused to a hemagglutinin (HA) tag sequence followed by a tobacco etch virus (TEV) protease cleavage site, pCXN2/HA-TEV-NS4B, was previously described (49). Huh-7.5.1-8 cells were transfected with pCXN2/HA-TEV-NS4B using FuGENE 6 transfection reagent (Roche Applied Science) and grown in the presence of 500 μg/ml of G418. G418-resistant cells were cloned by limiting dilution, and expression of HA-tagged NS4B protein in each clone was confirmed by immunoblotting with a rat anti-HA monoclonal antibody (clone 3F10; Roche Applied Science). Similarly, Huh-7.5.1-8 cells were transfected with a backbone plasmid, a modified version of pCXN2 (50, 51). The resultant G418-resistant cells were cloned and used as a negative control.

Immunofluorescence analysis. Cells grown on collagen-coated coverslips (Asahi Glass Co., Ltd., Japan) were fixed with 4% paraformaldehyde phosphate buffer solution (Wako Pure Chemical Industries, Ltd.) for 15 min at room temperature. After being washed with 30 mM glycine in PBS, the cells were permeabilized with 0.2% Triton X-100 in PBS for 10 min at room temperature and then blocked with 3% (wt/vol) bovine serum albumin (BSA) in PBS. The cells were incubated with the anti-HA rat monoclonal antibody diluted 1:500 with 1% (wt/vol) BSA in PBS followed by an Alexa Fluor 488 goat anti-rat IgG(H+L) antibody (Life Technologies Corp.) diluted 1:300 with the same solution. The cells were mounted with ProLong Diamond antifade mountant with 4′,6-diamidino-2-phenylindole (DAPI) (Life Technologies Corp.) and observed using a confocal microscope (LSM 700; Carl Zeiss Microscopy, GmbH, Jena, Germany) equipped with an oil immersion objective lens (Plan-Apochromat 40×/1.4 oil DIC M27; Carl Zeiss Microscopy, GmbH).

Preparation of and infection with HCVpp. HCV pseudoparticles (HCVpp) were prepared as described previously (52, 53) with slight modifications. Briefly, HEK293T cells were transfected with a Gag-Pol packaging plasmid (Gag-Pol 5349), a reporter (luciferase) plasmid (Luc 126), and a pcDNA3.1(+) (Life Technologies Corp.)-based expression plasmid that encodes HCV envelope proteins (E1 and E2) of the JFH-1 strain (genotype 2a) or the TH strain (54) (genotype 1b) for 24 h using the

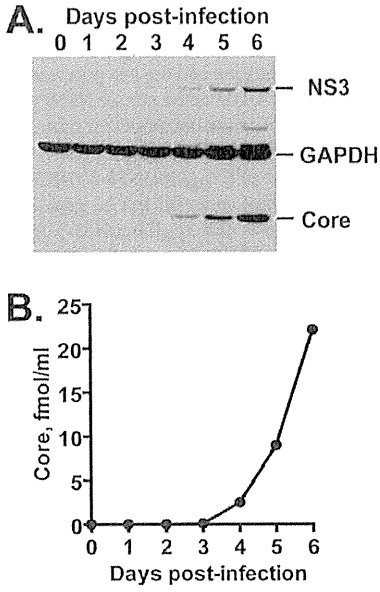

FIG 2 HCV production in Huh-7.5.1-8 cells grown under serum-free conditions. Huh-7.5.1-8 cells were infected with HCV JFH-1 and then cultured in serum-free medium. (A) The cells were harvested at the indicated time points. Each cell lysate (15 μg of protein) was subjected to immunoblotting for core, NS3, and GAPDH proteins. (B) Culture supernatants were harvested at the indicated time points. The amount of secreted viral particles in each supernatant was determined by measuring the amount of core protein by ELISA. The results from one of two independent experiments with similar results are shown.

X-treme Gene HP DNA transfection reagent (Roche Applied Science), and then the medium was replaced with serum-free medium that contained 0.1 mM nonessential amino acids. HCVpp-containing medium was collected after additional 24 to 36 h of culture and used as HCVpp stock. In parallel, HEK293T cells were similarly transfected, except that the envelope protein-expressing plasmid was replaced with pcDNA3.1(+), and their culture medium was used as a negative control. For infection, Huh-7.5.1-8 cells were plated at 6×10^4 cells per well of a 48-well plate and grown in serum-free medium for 2 days. The cells were then infected with HCVpp for 6 h at 37°C. After being washed, the cells were grown in complete medium for an additional 3 days and assayed for luciferase activity.

Other methods. Protein concentrations were measured using the bicinchoninic acid (BCA) protein assay reagent (Thermo Fisher Scientific, Inc., Waltham, MA, USA) with BSA as a standard. The amount of viral core protein in a culture supernatant, which is the hallmark of the secreted virus level, was quantified using the Ortho HCV antigen enzyme-linked immunosorbent assay (ELISA) (Ortho-Clinical Diagnostics, Inc., Raritan, NJ, USA). Cell viability was determined by using the XTT cell proliferation kit II (Roche Applied Science). The 50% inhibitory concentration (IC_{50}) was calculated by using the equation "log (inhibitor) versus normalized response" of the nonlinear regression model included in GraphPad Prism 5 (GraphPad Software, Inc., La Jolla, CA, USA). Statistical analysis was performed by Student's *t* test using the GraphPad calculator (QuickCalcs); differences with a *P* value of <0.05 were considered statistically significant.

RESULTS

Anti-HCV effect of YM-53601. We began to explore the role of the cholesterol biosynthetic pathway in the HCV life cycle by using an SQS inhibitor, YM-53601. We first examined whether HCV

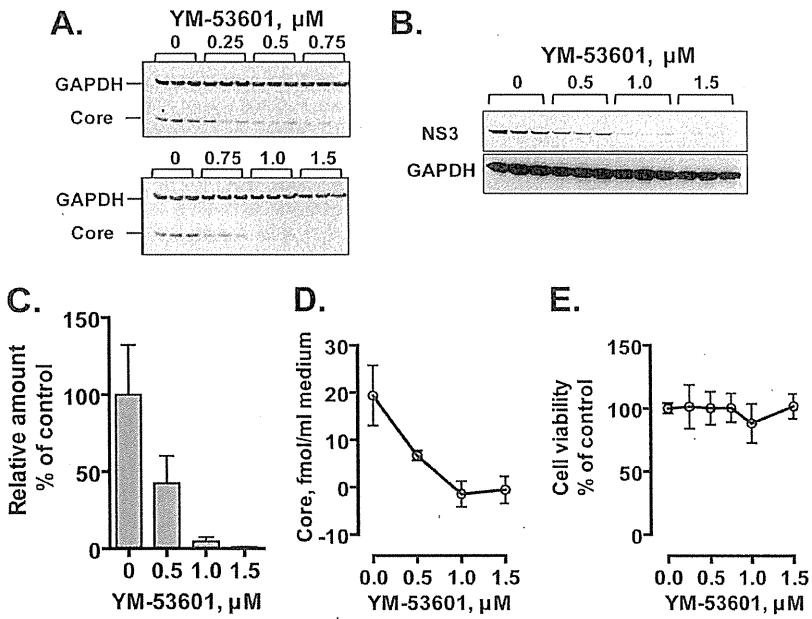

FIG 3 YM-53601 inhibits HCV production without affecting cell viability. Huh-7.5.1-8 cells were infected with HCV JFH-1 and then treated with increasing concentrations of YM-53601 (0 to 1.5 μM) in serum-free medium. The cells and culture supernatants were harvested on the fifth day postinfection. (A and B) An equal portion of each cell lysate was subjected to immunoblotting for core, NS3, and GAPDH proteins. The results from one representative experiment performed in triplicate are shown. Similar results were obtained in four independent experiments. For panel A, samples were run on two blots and are partially redundant. (C) Total RNA fractions were prepared from cells, and then viral and GAPDH RNAs were quantified by RT-qPCR analysis using specific primers for the core and GAPDH sequences, respectively. The amounts of viral RNA relative to that of GAPDH mRNA are expressed as a percentage of the control value and plotted as a function of the drug concentration. (D) The amount of secreted viral particles in each culture supernatant was determined by ELISA for the core protein and plotted as in panel C. (E) Cell viability was determined by XTT assay and expressed and plotted as in panel C. The data in each graph are means ± standard deviations (SD) for triplicate samples from one representative experiment. Similar results were obtained in two or more independent experiments.

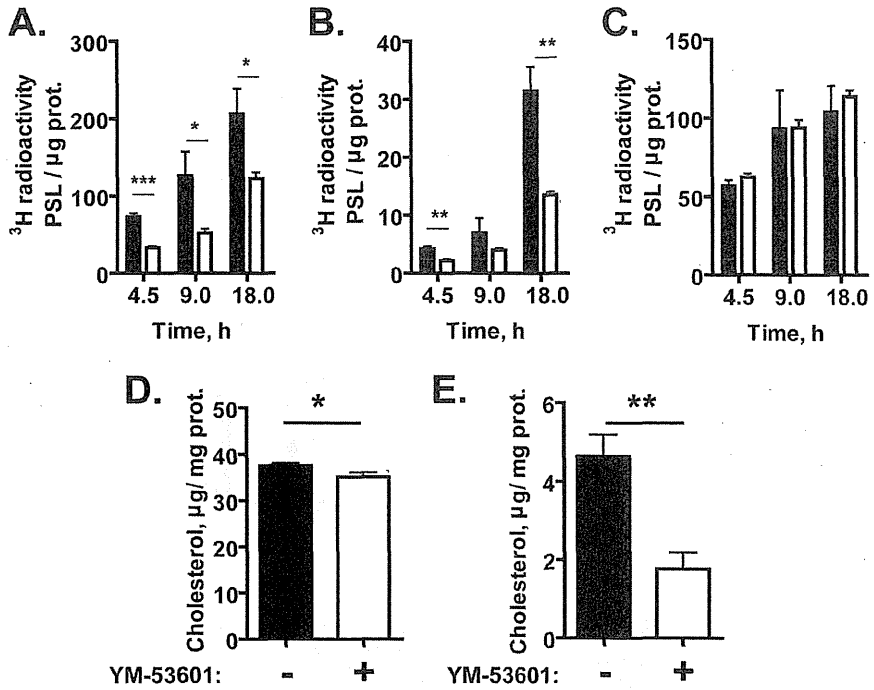

FIG 4 YM-53601 inhibits *de novo* synthesis of cholesterol and cholesteryl esters. (A to C) Huh-7.5.1-8 cells were pretreated with 1 µM YM-53601 (white bars) or its vehicle, DMSO (black bars), in serum-free medium for 24 h. The cells were subsequently labeled using [^{3}H]acetate in the same medium as for the pretreatment for the indicated periods of time. The lipid fractions were extracted from the cells and analyzed by TLC. The incorporation of [^{3}H]acetate into cholesterol (A), cholesteryl esters (B), and triglycerides (C) was quantified and expressed as photostimulated luminescence (PSL) values per µg cellular protein. (D and E) Huh-7.5.1-8 cells were treated with 1 µM YM-53601 (white bars) or DMSO (black bars) for 7 days in serum-free medium. The lipid fraction was extracted from the cells, and the contents of cholesterol (D) and cholesteryl esters (E) were determined. The values for cholesteryl esters (E) are expressed as the cholesterol content in the fraction. Data are means ± SD of triplicate samples from one representative experiment. Similar results were obtained in two independent experiments. *, $P < 0.05$; **$P < 0.01$; ***$P < 0.001$.

JFH-1 can replicate efficiently in Huh-7.5.1-8 cells grown under serum-free conditions where cellular cholesterol requirements are met only through *de novo* synthesis. The amounts of viral core and NS3 proteins in JFH-1-infected cells clearly increased from the fourth to sixth day postinfection, compared with that of GAPDH protein (Fig. 2A). Similarly, the amount of secreted viral particles increased during the time course (Fig. 2B). These results indicate that the virus replicates efficiently under the serum-free conditions.

We next examined the effect of YM-53601 on JFH-1 virus production in Huh-7.5.1-8 cells grown under serum-free conditions. The amounts of core (Fig. 3A) and NS3 (Fig. 3B) proteins relative to that of GAPDH protein in infected cells were decreased by the drug treatment in a dose-dependent manner and nearly reached the background level at ≥1 µM. Similarly, the relative amount of intracellular viral RNA (Fig. 3C) and the amount of secreted viral particles (Fig. 3D) were decreased by the drug treatment. The IC_{50} for virus secretion calculated from multiple experiments was 0.16 ± 0.10 µM ($n = 4$). In contrast, cell viability was not affected by the drug at up to 1.5 µM (Fig. 3E). These results indicate that YM-53601 inhibits HCV production in Huh-7.5.1-8 cells without affecting cell viability. The drug also inhibited HCV production from Huh-7.5.1-8 cells grown in serum-containing medium (data not shown) with a slightly higher value of IC_{50} (0.57 ± 0.66 µM; $n = 4$).

To evaluate the effect of YM-53601 on the infectivity of progeny virus, we inoculated naive Huh-7.5.1-8 cells with culture supernatants that contained viral particles secreted from drug-treated (1 µM) and untreated cells. When the inoculum dose was adjusted to contain an equal amount of core protein, these supernatants yielded almost the same amount of progeny viral particles (data not shown), indicating that the drug does not alter the infectivity of progeny virus.

YM-53601 inhibits cholesterol biosynthesis. To test whether YM-53601 inhibits *de novo* synthesis of cholesterol, we pretreated Huh-7.5.1-8 cells with a 1 µM concentration of the drug in serum-free medium for 24 h and then labeled them with [^{3}H]acetate for up to 18 h in the same medium. The drug treatment led to a 40 to 60% reduction in the incorporation of [^{3}H]acetate into cellular cholesterol (Fig. 4A) and its major metabolites, cholesteryl esters (Fig. 4B), compared with the control treatment. In contrast, the incorporation into triglycerides was not affected by the drug (Fig. 4C), indicating a specific effect of YM-53601 on cholesterol biosynthesis. We also determined the cellular contents of cholesterol and cholesteryl esters in Huh-7.5.1-8 cells treated with 1 µM YM-53601 in serum-free medium. The contents of cholesterol (Fig. 4D) and cholesteryl esters (Fig. 4E) in the drug-treated cells were significantly decreased to 93.5% and 38.0%, respectively, of those in the untreated cells. Collectively, these results confirm that YM-53601 inhibits *de novo* cholesterol biosynthesis at the antiviral concentrations.

SQS is an anti-HCV target. To further test whether cellular

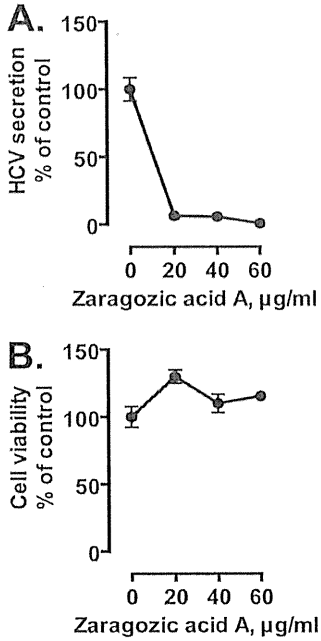

FIG 5 Anti-HCV effect of another SQS inhibitor, zaragozic acid A. Huh-7.5.1-8 cells were infected with HCV JFH-1 and then treated with 0 to 60 μg/ml of zaragozic acid A for 4 days. In this experiment, drug treatment was performed in complete medium because the drug was toxic to cells in serum-free medium. (A) The amount of secreted viral particles in each culture supernatant was determined by ELISA for the core protein. (B) Cell viability was determined by XTT assay. Data in each graph are expressed as a percentage of the control value (without the drug) and are means ± SD for triplicate samples from one representative experiment. Similar results were obtained in two independent experiments. Some error bars are not visible due to their small sizes.

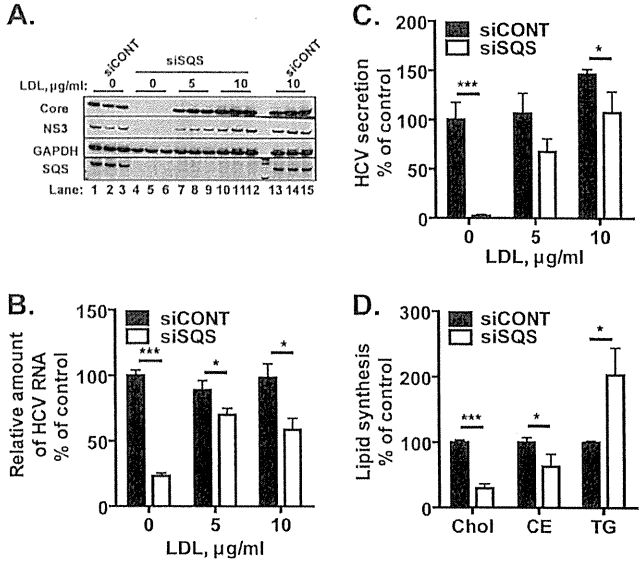

FIG 6 Anti-HCV effect of siRNA-mediated knockdown of SQS and its reversal by the addition of LDL. (A to C) Huh-7.5.1-8 cells were infected with HCV JFH-1 and then incubated in complete medium. On the first day postinfection, the cells were transfected with an siRNA for SQS (siSQS) or a control siRNA (siCONT), and then they were further incubated in serum-free medium that contained 0, 5, and 10 μg/ml of LDL for 4 days. (A) An equal portion of each cell lysate was subjected to immunoblotting for core, NS3, GAPDH, and SQS proteins. The results from one representative experiment performed in triplicate are shown. Similar results were obtained in two independent experiments. (B) Total RNA fractions were isolated from siSQS-transfected (white bars) or siCONT-transfected (black bars) cells, and then HCV RNA was quantified by RT-qPCR analysis using specific primers for the NS5B sequence. The amount of viral RNA relative to that of GAPDH mRNA is expressed as a percentage of the control value (siCONT without LDL) and plotted as a function of the LDL concentration. (C) The amount of secreted viral particles in each culture supernatant was determined by ELISA for the core protein. The concentration of core protein is expressed and plotted as in panel B. (D) Huh-7.5.1-8 cells were transfected with siSQS (white bars) or siCONT (black bars) and subsequently labeled using [^{3}H]acetate in serum-free medium for 18 h. The lipid fractions were extracted from the cells and analyzed by TLC. The incorporation of [^{3}H]acetate into cholesterol (Chol), cholesteryl esters (CE), and triglycerides (TG) was quantified and expressed as a percentage of the control value. Note that the value for cholesteryl esters of siSQS-transfected cells includes in part the incorporation of unidentified metabolites located immediately below the cholesteryl esters on a TLC plate. These metabolites accumulated only in siSQS-transfected cells for unknown reasons. The data in panels B, C, and D are means ± SD for triplicate samples from one representative experiment. Similar results were obtained in at least two independent experiments. *, $P < 0.05$; ***$P < 0.001$.

SQS is important for HCV production, we first investigated the effects of another SQS inhibitor, zaragozic acid A (squalestatin S1), on HCV production. The drug decreased the amounts of core and NS3 proteins and viral RNA (data not shown) and progeny virus production (Fig. 5A) without affecting cell viability (Fig. 5B), indicating that zaragozic acid A inhibits HCV production as well as YM-53601.

We next investigated the effect of siRNA-mediated knockdown of SQS on HCV production. Huh-7.5.1-8 cells were infected with HCV JFH-1 and then transfected with either an siRNA against SQS (siSQS) or a control siRNA (siCONT). Transfection with siSQS resulted in almost complete depletion of cellular SQS compared with transfection with siCONT (Fig. 6A, bottom row). The amounts of core and NS3 proteins relative to GAPDH protein in the siSQS-transfected cells were markedly lower than those in the control cells (Fig. 6A, compare lanes 4 to 6 with lanes 1 to 3). The relative amounts of intracellular viral RNA (Fig. 6B, left pair of bars) and secreted viral particles (Fig. 6C, left pair of bars) were also decreased in the siSQS-transfected cells. A similar antiviral effect was observed with another siRNA for SQS (a Stealth RNAi siRNA, HSS103616) (data not shown). These results indicate that siRNA-mediated knockdown of SQS leads to reduced HCV production.

A metabolic labeling experiment with [^{3}H]acetate confirmed that transfection with siSQS causes a specific decrease in cholesterol biosynthesis (Fig. 6D). To rescue the defective cholesterol biosynthesis, we added LDL (final concentrations, 5 and 10 μg/ml) to the medium of HCV-infected cells after siSQS transfection. The inhibition of virus production by siSQS was reversed by the addition of LDL (Fig. 6A to C), suggesting that the antiviral effect is attributable to a decrease in cellular contents of cholesterol and/or cholesteryl esters. Consistent with this, the inhibition of virus production by YM-53601 was also reversed significantly by the addition of LDL as judged by intracellular viral protein levels (Fig. 7).

Collectively, these results demonstrate that SQS is a potential target for anti-HCV strategies.

An ACAT inhibitor does not show an anti-HCV effect. The degree of decrease in the cholesteryl ester content after treatment with YM-53601 (Fig. 4E) was substantially higher than that in the

zjv00415/zjv0052d15z | xppws | S=1 | 12/10/14 | 12:17 | 4/C Fig: 10 | ArtID: 03385-14 | NLM: research-article | CE: sj

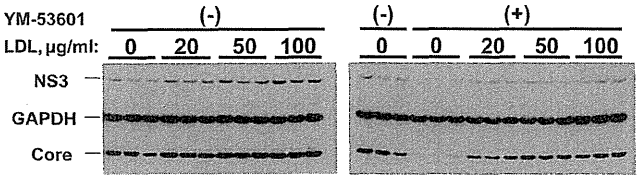

FIG 7 The anti-HCV effect of YM-53601 is significantly reversed by LDL. Huh-7.5.1-8 cells were infected with HCV JFH-1 and then treated with 1 μM YM-53601 or DMSO in serum-free medium that contained 0 to 100 μg/ml of LDL for 5 days. An equal portion of each cell lysate was subjected to immunoblotting for core, NS3, and GAPDH proteins. The results from one representative experiment performed in triplicates are shown. Similar results were obtained in two independent experiments.

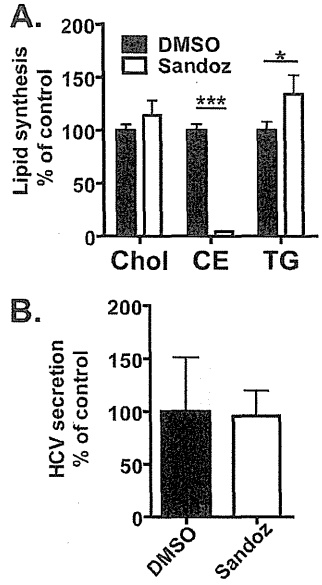

FIG 8 An ACAT inhibitor, Sandoz 58-035, does not exhibit an anti-HCV effect. (A) Huh-7.5.1-8 cells were pretreated with 30 μM Sandoz 58-035 or its vehicle, DMSO, in serum-free medium for 24 h. The cells were subsequently labeled using [^{3}H]acetate in the same medium as for the pretreatment for 18 h. The lipid fractions were extracted from cells and separated by TLC. The incorporation of [^{3}H]acetate into cholesterol (Chol), cholesteryl esters (CE), and triglycerides (TG) was quantified and expressed as a percentage of the control value. (B) Huh-7.5.1-8 cells were infected with HCV JFH-1 and then treated with Sandoz 58-035 or DMSO (control) under the same conditions as described above. The culture supernatants were harvested on the fifth day postinfection. The amount of secreted viral particles in each culture supernatant was determined by ELISA for the core protein and is expressed as a percentage of the control value. Data in each graph are means ± SD for triplicate samples from one representative experiment. Similar results were obtained in two independent experiments. *, $P < 0.05$; ***$P < 0.001$.

cholesterol content (Fig. 4D), raising the possibility that biosynthesis of cholesteryl esters is more important for HCV production than that of cholesterol. To test this possibility, we examined the effect of Sandoz 58-035, an inhibitor of acyl-CoA:cholesterol acyltransferase (ACAT) that catalyzes the biosynthesis of cholesteryl esters from cholesterol and fatty acyl-CoA, on HCV production. A metabolic labeling experiment with [^{3}H]acetate verified that treatment with 30 μM Sandoz 58-035 inhibits cholesteryl ester synthesis but not cholesterol and triglyceride syntheses in Huh-7.5.1-8 cells grown in serum-free medium (Fig. 8A). When Huh-7.5.1-8 cells were infected with HCV JFH-1 and then treated with either 30 μM Sandoz 58-035 or DMSO (control) in serum-free medium, virus secretion from the drug-treated cells was similar to that from the control cells (Fig. 8B). Taken together with the results shown in Fig. 3 and 4, these results suggest that biosynthesis of cholesterol, but not that of cholesteryl esters, is important for HCV production.

YM-53601 inhibits RNA replication of HCV JFH-1. To investigate which stages of the HCV life cycle are targeted by YM-53601, we conducted a transient-replication assay using a subgenomic replicon, SGR-JFH1/Luc (45). When cells are transfected with this replicon RNA, the self-encoded viral RNA replicase (NS3-NS5B) is expressed under the control of the EMCV IRES and then amplifies the replicon in the cells. The replicon also encodes luciferase translated under HCV IRES control, thereby allowing quantitation of viral RNA replication and translation activities via luciferase expression. Parallel transfection with a replication-incompetent mutant replicon, SGR-JFH1/Luc-GND (45), enables estimation of the level of replication-independent luciferase expression from the input replicon. As shown in Fig. 9A, luciferase activity in the wild-type replicon-transfected cells reached its peak at 47 h posttransfection and then declined. In the presence of YM-53601, the peak activity was decreased to approximately half of that in the control cells. The mutant replicon yielded very low luciferase activity irrespective of the drug treatment, confirming that the activity yielded by the wild-type replicon at 23 to 71 h posttransfection was dependent on viral RNA replication. Multiple experiments showed that the drug treatment lowered the peak luciferase activity to 52.6% ± 25.3% ($n = 5$; $P = 0.014$) of the control activity.

To test whether YM-53601 inhibits HCV IRES-dependent translation, we transfected drug-pretreated Huh-7.5.1-8 cells with the replication-incompetent mutant replicon SGR-JFH1/Luc-GND and then monitored luciferase expression in the presence of the drug for up to 21 h. Because the replicon cannot be replicated, luciferase activity yielded by the mutant replicon is attributable exclusively to HCV IRES-dependent translation and reflects the residual amount of the input replicon RNA. As shown in Fig. 9B, luciferase activity in the drug-treated cells and untreated control cells reached its peak at 3 h posttransfection and then declined. During the time course, the activity in the drug-treated cells was not lower, but rather was higher, than the activity in the control cells. Furthermore, the level of NS3 protein that was expressed from the mutant replicon changed similarly in the drug-treated and control cells, reaching its peak at 3 to 6 h posttransfection (Fig. 9C). Thus, it appears unlikely that YM-53601 impairs HCV IRES-dependent translation or viral RNA and NS protein stability.

Taken together, these results suggest that YM-53601 inhibits the RNA replication of HCV JFH-1.

YM-53601 does not affect the cellular distribution of NS4B protein. It is possible that YM-53601 alters the formation of the HCV-specific ultrastructure termed the membranous web, which serves as a scaffold for the viral RNA replication complex (55, 56), thereby inhibiting viral RNA replication. To test this possibility, we treated Huh-7.5.1-8 cells stably expressing HA-tagged NS4B protein with YM-53601 for 3 days in serum-free medium. It has been shown that the membranous web is induced by NS4B protein alone (55, 57) and appears as NS4B-accumulating foci or dots under fluorescence microscopy (58, 59). We found small intense foci that were detected with an anti-HA antibody in non-drug-

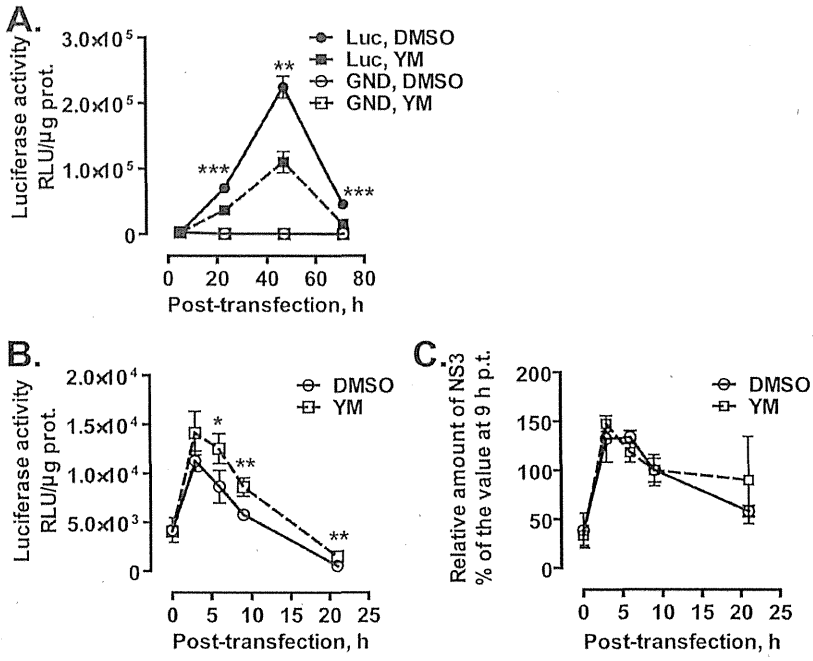

FIG 9 YM-53601 inhibits HCV RNA replication of HCV JFH-1. (A) Transient-replication assay using JFH-1 subgenomic replicons. Huh-7.5.1-8 cells were transfected with SGR-JFH1/Luc (closed symbols) or SGR-JFH1/Luc-GND (open symbols) RNAs by electroporation and then placed in serum-free medium. At 5 h posttransfection, YM-53601 (final concentration, 1.5 μM) (squares and dashed line) or DMSO (circles and solid line) was added to the medium. The cells were harvested at the indicated time points (posttransfection) and assayed for luciferase activity. (B and C) Huh-7.5.1-8 cells were pretreated with 1.5 μM YM-53601 or DMSO in serum-free medium for 42 h and then transfected with SGR-JFH1/Luc-GND RNA by lipofection. After transfection, the cells were further treated in the same medium and harvested at the indicated time points. (B) The cells were lysed and assayed for luciferase activity. (C) An equal amount of protein (10 μg/lane) in each cell lysate was subjected to immunoblotting for NS3 and GAPDH proteins, and each protein band was quantified. The relative amount of NS3 protein was calculated by dividing its intensity by that of GAPDH protein in the same lane. Data are expressed as a percentage of the relative amount at 9 h posttransfection. The value at 9 h posttransfection was not significantly different between the drug-treated and untreated cells (data not shown). Data in each graph are means ± SD for triplicate samples from one representative experiment. Similar results were obtained in at least two independent experiments. Statistical analysis was performed between drug-treated and control cells harboring the same replicon. *, $P < 0.05$; **$P < 0.01$; ***$P < 0.001$.

F10 treated cells (Fig. 10C) and are similar to the NS4B foci previously reported (58, 60, 61). The foci were not detected in Huh-7.5.1-8 cells transfected with a backbone plasmid (Fig. 10A and B). Drug treatment resulted in no apparent alteration in NS4B foci (Fig. 10D) or the expression level of NS4B protein (data not shown), suggesting that the drug does not grossly alter the formation of the membranous web by NS4B protein.

RNA replication of HCV genotype 1b is not inhibited by YM-53601. To examine whether YM-53601 is able to inhibit viral RNA replication of HCV strains other than the JFH-1 strain (genotype 2a), we performed a transient-replication assay using a subgenomic replicon of the Con-1 strain (genotype 1b), FK-I_{389}Luci/NS3-3′/NK5.1 (46), and its replication-incompetent mutant, FK-I_{389}/Luci/NS3-3′/NK5.1/ΔGDD. Consistent with the previous report (46), time-dependent luciferase expression in the Con-1 replicon-transfected cells exhibited a downward-sloping pattern: luciferase activity at early time points (2.5 to 7 h posttransfection) F11 was higher than the activity at later time points (Fig. 11A). At the early time points, the activity in the wild-type replicon-transfected cells was lower than the activity in the mutant replicon-transfected cells, indicating that RNA replication is too low to be detected at these early points. Afterwards, the activity in the wild-type replicon-transfected cells stayed higher than the activity in the mutant replicon-transfected cells, indicating that the difference between these activities was attributed to viral RNA replication. Unlike in the case of the JFH-1 replicon, treatment with YM-53601 did not lower RNA replication-dependent luciferase expression but rather enhanced it. From multiple experiments, the luciferase activity in the drug-treated cells at 46 to 50 h posttransfection was 284% ± 124% ($n = 4$) of the control activity.

To increase the impact of YM-53601, we performed a similar transient-replication assay using Huh-7.5.1-8 cells pretreated with the drug in serum-free medium for 2 days. Unexpectedly, serum-free preculture before transfection led to an overall decrease of two orders of magnitude in luciferase expression (Fig. 11B). In untreated control cells, RNA replication-dependent luciferase expression (i.e., the difference between the activity yielded by the wild-type replicon and that yielded by the mutant replicon) was not clearly found until 47 h posttransfection (compare black bars with hatched bars). However, RNA replication-dependent luciferase expression in drug-treated cells was found at and after 7 h posttransfection (compare gray bars with white bars) and was slightly higher than that in the untreated cells. Thus, the RNA replication-dependent luciferase expression does not appear to be inhibited by even a prolonged drug treatment.

Taken together, these results suggest that RNA replication of the Con-1 strain is not inhibited by YM-53601.

Entry of HCVpp of genotype 2a but not genotype 1b is blocked by YM-53601. To further investigate how YM-53601 blocks HCV production, we conducted an entry assay for HCV

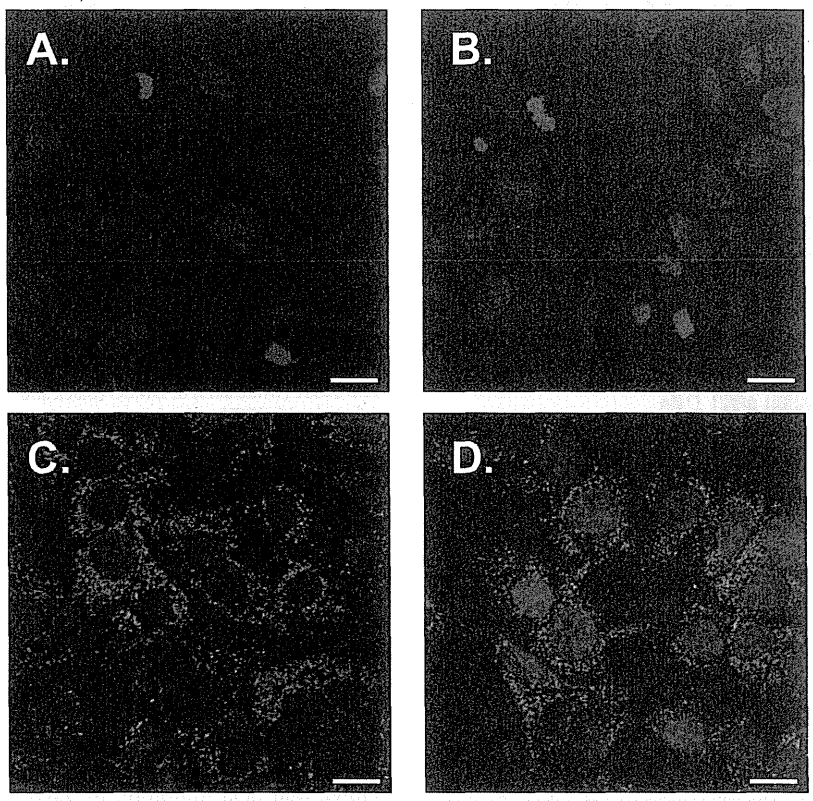

COLOR

FIG 10 YM-53601 does not affect NS4B foci in Huh-7.5.1-8 cells. Huh-7.5.1-8 cells that were stably transfected with modified pCXN2 (A and B) or pCXN2/HA-TEV-NS4B (C and D) were grown on coverslips and treated with 1.5 μM YM-53601 (B and D) or DMSO (A and C) in serum-free medium for 3 days. The cells were fixed and subjected to immunofluorescence analysis using confocal microscopy. HA-tagged NS4B protein was detected with a rat anti-HA antibody followed by an Alexa Fluor 488-conjugated anti-rat antibody (green), and the nucleus was stained with DAPI (blue). Scale bars represent 20 μm.

pseudoparticles (HCVpp), which enter cells by using HCV envelope protein but replicate via a retroviral system (52). Although YM-53601 was added to cells after infection (Fig. 3 and 7), a block at the step of entry of progeny virus is possible because more than one round of infection can occur under our experimental conditions. Huh-7.5.1-8 cells were preincubated with YM-53601 in serum-free medium for 2 days and then infected in the presence of the drug with HCVpp harboring envelope glycoproteins from the JFH-1 strain. The cells were thereafter incubated in the absence of the drug for 3 days, and luciferase activity, reflecting the degree of HCVpp entry into host cells, was measured. Treatment with YM-53601 reduced luciferase activity to less than 50% of the activity in untreated cells (Fig. 12, left two bars). Infection with mock HCVpp prepared without envelope glycoproteins did not yield luciferase activity (<3 relative light units [RLU]/μg protein), confirming that luciferase expression is dependent on the envelope glycoproteins (data not shown). When the drug was added only at HCVpp infection, no reduction in the luciferase expression was found (Fig. 12, third bar from left), suggesting that the drug targets cells but not HCVpp. These results are consistent with the previous report showing partial cholesterol dependency of HCV entry (14). Similarly, we tested the effect of the drug on HCVpp harboring envelope glycoproteins from genotype 1b HCV (strain TH). Drug treatment before and during infection or only during infection did not significantly alter luciferase expression (Fig. 12, right three bars). Taken together, these results suggest that YM-53601 blocks entry of HCV genotype 2a but not that of genotype 1b.

F12

DISCUSSION

The main aim of this study was to elucidate the importance of the committed pathway of cholesterol biosynthesis in the HCV life cycle. We have shown that three types of SQS inhibitor, YM-53601 (Fig. 3), zaragozic acid A (Fig. 5), and siSQS (Fig. 6), inhibited HCV JFH-1 production in Huh-7.5.1-8 cells in a similar manner. In particular, YM-53601 exerted an antiviral effect without remarkable cell toxicity. The antiviral effect of SQS inhibition was reversed by the addition of LDL (Fig. 6 and 7), indicating that the effect is attributable to cellular cholesterol and/or cholesteryl ester deficiencies (Fig. 4 and 6). Unlike YM-53601, no antiviral effect was observed with the ACAT inhibitor Sandoz 58-035 (Fig. 8), suggesting that synthesis of cholesterol rather than that of cholesteryl esters is important for HCV production. From these findings, we conclude that the committed pathway of cholesterol biosynthesis that begins with squalene synthesis (Fig. 1) plays an important role in the HCV life cycle. This conclusion is consistent with recent studies showing that inhibition of oxidosqualene cyclase, lanosterol C_{14}-demethylase, 24-dehydrocholesterol reductase, 7-dehydrocholesterol reductase, and SQS (discussed below) leads to decreased HCV production (31–33, 62). Furthermore, we propose that SQS is a potential target for anti-HCV strategies because all the SQS inhibitors tested in this study exerted anti-HCV effects.

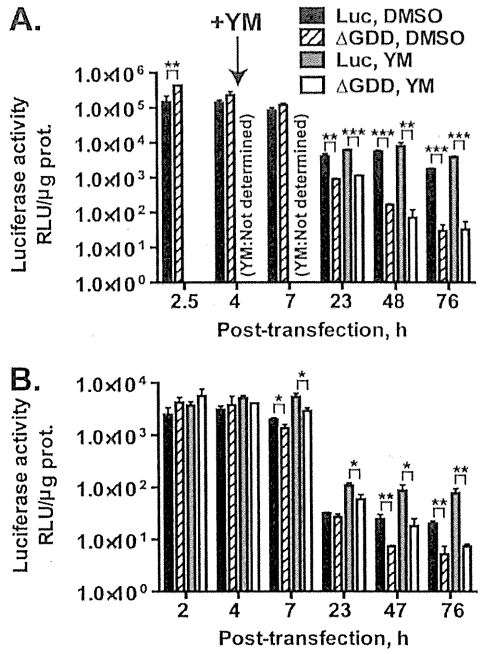

FIG 11 YM-53601 does not inhibit transient replication of Con-1 subgenomic replicons. (A) Huh-7.5.1-8 cells were transfected with FK-I_{389}Luci/NS3-3′/NK5.1 (Luc) (black and gray bars) or FK-I_{389}/Luci/NS3-3′/NK5.1/ΔGDD (ΔGDD) (hatched and white bars) RNAs by electroporation and then placed in serum-free medium. At 4 h posttransfection, YM-53601 (YM) (final concentration, 1.5 μM) (gray and white bars) or DMSO (black and hatched bars) was added to the medium. The cells were harvested at the indicated time points (posttransfection) and assayed for luciferase activity. (B) Huh-7.5.1-8 cells were pretreated with 1.5 μM YM-53601 or DMSO in serum-free medium for 47 h. The cells were transfected with FK-I_{389}Luci/NS3-3′/NK5.1 or FK-I_{389}/Luci/NS3-3′/NK5.1/ΔGDD RNAs and then further treated in the same medium. The cells were harvested at the indicated time points (posttransfection) and assayed for luciferase activity. Bars are as described for panel A. Data in each graph are means ± SD for triplicate samples from one representative experiment and are presented on a logarithmic scale because of large range of values. Some error bars are not visible due to their small sizes. Similar results were obtained in at least two independent experiments. *, $P < 0.05$; **$P < 0.01$; ***$P < 0.001$.

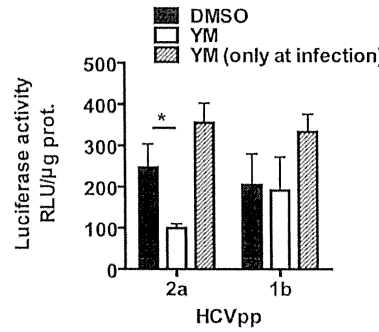

FIG 12 YM-53601 blocks entry of genotype 2a, but not genotype 1b, HCVpp. Huh-7.5.1-8 cells were grown in serum-free medium that contained 1.5 μM YM-53601 (white bars) or DMSO (black and hatched bars) for 2 days and then infected with HCVpp in the presence (white and hatched bars) or absence (black bars) of the drug. The cells were further grown in complete medium without the drug for 3 days and assayed for luciferase activity. Data are means ± SD for triplicate samples from one representative experiment. Similar results were obtained in two independent experiments. *, $P < 0.05$.

It has been reported that the peak plasma concentration of YM-53601 is 0.92 μg/ml (approximately 2.5 μM) after oral administration in rats at a dose with a cholesterol-lowering effect (38, 63). This concentration is roughly close to the IC_{50} of YM-53601 for HCV production in the presence of serum. Thus, YM-53601 might exert an anti-HCV effect *in vivo*.

Using a transient-replication assay (Fig. 9A) and the HCVpp system (Fig. 12), we found that suppression of HCV RNA replication and entry is involved in the antiviral mechanism of YM-53601 against JFH-1 virus. However, the degrees of suppression of these processes were at most approximately 50% in our assays. Accordingly, these mechanisms alone may not explain the more severe inhibition of HCV production observed in the HCV cell culture system (Fig. 3). Possibly, some steps in the HCV life cycle other than RNA replication and entry might be sensitive to the drug. Alternatively, some steps which are not reproduced in the subgenomic replicon and HCVpp systems might be more sensitive to the drug.

YM-53601 inhibited transient RNA replication of the subgenomic reporter replicon from the JFH-1 strain (genotype 2a) (Fig. 9A) but somewhat enhanced that of the subgenomic replicon from the Con-1 strain (genotype 1b) (Fig. 11). Similarly, the drug inhibited entry of genotype 2a, but not genotype 1b, HCVpp (Fig. 12). These findings raise the possibility that the cholesterol requirement for HCV RNA replication and entry varies among virus genotypes. Consistent with our results, previous studies have shown that SQS inhibition by zaragozic acid A leads to an enhancement of genotype 1b RNA replication (28, 31). This proviral effect appears to be caused by an increase in geranylgeranyl pyrophosphate, which is required for geranylgeranylation of a viral host factor and elevated expression of HMG-CoA reductase (31). In the case of genotype 2a, the proviral effect might be overwhelmed by antiviral effect caused by cholesterol depletion. Interestingly, genotype-specific inhibition of HCV RNA replication was also observed with inhibitors of sphingomyelin biosynthesis (19, 64, 65). Thus, major components of lipid rafts, i.e., cholesterol and sphingomyelin, appear to be similar in that they both contribute to HCV RNA replication in a genotype-dependent manner. AQ: B

During preparation of this paper, Park et al. reported that siRNAs against farnesyl-diphosphate farnesyltransferase 1 (another name for SQS) and YM-53601 impair propagation of the HCV Jc1 strain (genotype 2a) in Huh-7.5 cells (62). They suggested that these agents target viral RNA replication by using a luciferase-encoding full genomic replicon of the JFH-1 strain and genotype 2a subgenomic replicon cells. These findings are consistent with our results. However, their finding that the viral RNA level in genotype 1b subgenomic replicon cells is decreased by SQS knockdown appears to argue against our results, as we could not find any antiviral effect of YM-53601 on genotype 1b RNA replication (Fig. 11). Although the reason for this discrepancy is currently unknown, differences in the culture conditions (serum-containing medium versus serum-free medium), replication assay (RT-qPCR versus reporter), methods of SQS inhibition (siRNA versus drug), and origin of the subgenomic replicon might be involved. In any case, we should evaluate the effects of SQS inhibitors on the complete life cycle of HCV genotype 1b when cell culture systems capable of supporting its growth are developed.

Our data suggest that biosynthesis of cholesterol, rather than that of cholesteryl esters, is important for HCV production (Fig. 8). Treatment with YM-53601 led to only a slight reduction in cholesterol levels (Fig. 4D) but severely impaired HCV production, implying that the drug selectively decreases relatively minor but specific pools of cellular cholesterol that are important for HCV production. Given that lipid rafts may serve as sites for viral RNA replication (15–17), assembly (19, 20), and virus entry (14, 19, 66), one scenario is that YM-53601 might selectively decrease lipid raft-associated cholesterol, thereby perturbing these processes. Consistent with this proposition, inhibition of SQS in prostate cancer cells results in a decrease of raft-associated cholesterol rather than nonraft cholesterol (67). On the other hand, a recent study has shown that purified double-membrane vesicles containing active HCV RNA replication complexes are highly enriched with cholesterol (68), although they originate from the ER, which is poor in cholesterol (69). It has also been shown that cholesterol depletion from the double-membrane vesicles decreases viral RNA levels associated with them, suggesting that cholesterol is an important structural component of HCV RNA replication complexes. Cholesterol biosynthesis (70) and HCV RNA replication (71, 72) both occur in the ER, and some cholesterol biosynthetic enzymes, including SQS, are partially copurified with components of HCV RNA replication complexes (73), implying that the cholesterol biosynthetic machinery might be closely associated with HCV RNA replication complexes in the ER. Thus, another scenario is that YM-53601 might decrease newly synthesized ER cholesterol pools, which might be preferentially used for structural components of membrane-bound viral RNA replication complexes. Preferential use of newly synthesized cholesterol in the formation of envelope membranes of human immunodeficiency virus has been found (74). Note that we could not detect any impact of YM-53601 on the morphology of NS4B-induced foci, which are considered scaffolds of viral RNA replication complexes, under fluorescence microscopy (Fig. 10). Thus, alteration in the structure of RNA replication complexes caused by YM-53601, if any, might be found at the ultrastructural level.

AQ: C

Our data provide evidence that the committed pathway of cholesterol biosynthesis is important for HCV production, consistent with recent studies (31–33, 62). Moreover, we found that biosynthesis of cholesterol, but not of cholesteryl esters, is important for this process. The identity of the cholesterol pools required for HCV production and the molecular mechanisms underlying the cholesterol requirement should be elucidated in future studies. Our data also provide concrete evidence that SQS is a potential anti-HCV target. Further studies are required to ascertain the anti-HCV activity of SQS inhibitors *in vivo*. SQS inhibitors are expected to exert fewer adverse effects on human cells than statins because SQS inhibitors lower cholesterol without depleting nonsterol isoprenoids (75, 76). For this reason, many compounds targeting SQS have been developed in the past by the pharmaceutical industry as potential cholesterol-lowering drugs for hypercholesterolemia. Thus, reevaluation of these compounds for potential anti-HCV activity might offer a time-saving and cost-effective approach for developing anti-HCV drugs.

ACKNOWLEDGMENTS

The pFK-I_{389}Luci/NS3-3′/NK5.1 and pFK-I_{389}neo/NS3-3′/NK5.1/ΔGDD plasmids were kind gifts from Ralf Bartenschlager. We thank Kiyoshi Kawasaki (Doshisha Woman's College) for useful suggestions and Toshiyuki Yamaji for technical assistance.

This study was supported by the National Cancer Center Research and Development Fund (grant no. 7 to M.F.) from the National Cancer Center of Japan, by Health and Labor Sciences research grants for research on hepatitis from the Ministry of Health, Labor and Welfare of Japan, and by Grants-in-Aid for Scientific Research (C) JSPS KAKENHI (grant no. 21590085 to K.S. and 23590104 to M.F.) from the Japan Society for the Promotion of Science.

REFERENCES

1. **World Health Organization.** 2014. Hepatitis C fact sheet no. 164. World Health Organization, Geneva, Switzerland. http://www.who.int/mediacentre/factsheets/fs164/en/.
2. **Ghany MG, Strader DB, Thomas DL, Seeff LB.** 2009. Diagnosis, management, and treatment of hepatitis C: an update. Hepatology **49:**1335–1374. http://dx.doi.org/10.1002/hep.22759.
3. **Alexopoulou A, Papatheodoridis GV.** 2012. Current progress in the treatment of chronic hepatitis C. World J Gastroenterol **18:**6060–6069. http://dx.doi.org/10.3748/wjg.v18.i42.6060.
4. **Doyle JS, Aspinall E, Liew D, Thompson AJ, Hellard ME.** 2013. Current and emerging antiviral treatments for hepatitis C infection. Br J Clin Pharmacol **75:**931–943. http://dx.doi.org/10.1111/j.1365-2125.2012.04419.x.
5. **Lawitz E, Sulkowski MS, Ghalib R, Rodriguez-Torres M, Younossi ZM, Corregidor A, DeJesus E, Pearlman B, Rabinovitz M, Gitlin N, Lim JK, Pockros PJ, Scott JD, Fevery B, Lambrecht T, Ouwerkerk-Mahadevan S, Callewaert K, Symonds WT, Picchio G, Lindsay KL, Beumont M, Jacobson IM.** 2014. Simeprevir plus sofosbuvir, with or without ribavirin, to treat chronic infection with hepatitis C virus genotype 1 in non-responders to pegylated interferon and ribavirin and treatment-naive patients: the COSMOS randomised study. Lancet **384:**1756–1765. http://dx.doi.org/10.1016/S0140-6736(14)61036-9.
6. **Schneider MD, Sarrazin C.** 2014. Antiviral therapy of hepatitis C in 2014: do we need resistance testing? Antiviral Res **105:**64–71. http://dx.doi.org/10.1016/j.antiviral.2014.02.011.
7. **Fraser CS, Doudna JA.** 2007. Structural and mechanistic insights into hepatitis C viral translation initiation. Nat Rev Microbiol **5:**29–38. http://dx.doi.org/10.1038/nrmicro1558.
8. **Grakoui A, Wychowski C, Lin C, Feinstone SM, Rice CM.** 1993. Expression and identification of hepatitis C virus polyprotein cleavage products. J Virol **67:**1385–1395.
9. **Bartenschlager R, Ahlborn-Laake L, Mous J, Jacobsen H.** 1993. Nonstructural protein 3 of the hepatitis C virus encodes a serine-type proteinase required for cleavage at the NS3/4 and NS4/5 junctions. J Virol **67:**3835–3844.
10. **Hijikata M, Mizushima H, Tanji Y, Komoda Y, Hirowatari Y, Akagi T, Kato N, Kimura K, Shimotohno K.** 1993. Proteolytic processing and membrane association of putative nonstructural proteins of hepatitis C virus. Proc Natl Acad Sci U S A **90:**10773–10777. http://dx.doi.org/10.1073/pnas.90.22.10773.
11. **Moradpour D, Penin F, Rice CM.** 2007. Replication of hepatitis C virus. Nat Rev Microbiol **5:**453–463. http://dx.doi.org/10.1038/nrmicro1645.
12. **Moradpour D, Gosert R, Egger D, Penin F, Blum HE, Bienz K.** 2003. Membrane association of hepatitis C virus nonstructural proteins and identification of the membrane alteration that harbors the viral replication complex. Antiviral Res **60:**103–109. http://dx.doi.org/10.1016/j.antiviral.2003.08.017.
13. **Felmlee DJ, Hafirassou ML, Lefevre M, Baumert TF, Schuster C.** 2013. Hepatitis C virus, cholesterol and lipoproteins—impact for the viral life cycle and pathogenesis of liver disease. Viruses **5:**1292–1324. http://dx.doi.org/10.3390/v5051292.
14. **Kapadia SB, Barth H, Baumert T, McKeating JA, Chisari FV.** 2007. Initiation of hepatitis C virus infection is dependent on cholesterol and cooperativity between CD81 and scavenger receptor B type I. J Virol **81:**374–383. http://dx.doi.org/10.1128/JVI.01134-06.
15. **Aizaki H, Lee KJ, Sung VM, Ishiko H, Lai MM.** 2004. Characterization of the hepatitis C virus RNA replication complex associated with lipid rafts. Virology **324:**450–461. http://dx.doi.org/10.1016/j.virol.2004.03.034.
16. **Shi ST, Lee KJ, Aizaki H, Hwang SB, Lai MM.** 2003. Hepatitis C virus RNA replication occurs on a detergent-resistant membrane that cofractionates with caveolin-2. J Virol **77:**4160–4168. http://dx.doi.org/10.1128/JVI.77.7.4160-4168.2003.